

This is to certify that the
thesis entitled

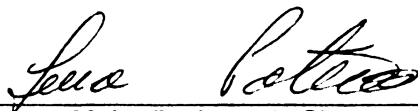
Petrologic Characterization of the Paleogene Arc, Costa Rica,
Central America

presented by

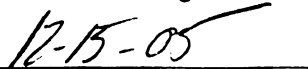
Beth Apple

has been accepted towards fulfillment
of the requirements for the

M.S. degree in Geological Sciences



Major Professor's Signature



Date

PLACE IN RETURN BOX to remove this checkout from your record.
TO AVOID FINES return on or before date due.
MAY BE RECALLED with earlier due date if requested.

DATE DUE	DATE DUE	DATE DUE

**PETROLOGIC CHARACTERIZATION OF THE PALEOGENE ARC,
COSTA RICA, CENTRAL AMERICA**

By

Beth Apple

A THESIS

**Submitted to
Michigan State University
in partial fulfillment of the requirements
for the degree of**

MASTER OF SCIENCE

Department of Geological Sciences

2005

ABSTRACT

Petrologic Characterization of Paleogene Arc, Costa Rica, Central America

By

Beth Apple

Lava clasts in Late Cretaceous to Eocene debris flows are manifestations of the earliest Costa Rican volcanic arc. This study characterizes the petrography and geochemistry of volcaniclasts from four sample locations (Punta Samara, Isla Paloma, Quebrada Buenaventura, and Playa Soley) to determine the subduction parameters for the primitive arc. Geochemical compositions of the primitive arc lavas are compared to samples from the volcanic front from the modern arc, concentrating on the Costa Rican and Nicaraguan segments. Selected trace element ratios of these clasts are used to infer subduction parameters including mantle source (Zr/Nb), degree of mantle melting (La/Yb), slab input (Ba/La), and sediment addition (Ba/Th, U/Th). The majority of primitive arc lava clasts originated from a depleted, mantle source (MORB-like), and have higher Zr/Nb ratios than those from modern central Costa Rica (CCR). However, two lava clasts have Zr/Nb ratios similar to CCR volcanics, indicating a contribution from a more enriched mantle source. The degree of mantle melting increases (low La/Yb) with an increase in slab signal (high Ba/La) in the primitive arc lava clasts, and these values are more similar to what is observed in modern western Nicaragua than in modern Costa Rica. This may be a reflection of a steeper angle of subduction offshore Costa Rica during the Late Cretaceous to the Eocene, possibly because the Farallon Plate was older, colder, and denser than the modern day Cocos Plate. The primitive arc lava clasts have high Ba/Th and low U/Th ratios indicating that the sediment subducted in the primitive arc likely had a carbonate component (high Ba/Th), but lacked the hemipelagic sediment component (high U/Th) that is subducted in the modern arc.

ACKNOWLEDGEMENTS

I have learned a great deal and had many invaluable experiences while working towards my M.S. There are many people to thank for this...

The Geological Society of America and Michigan State University College of Natural Science funded the travel to Costa Rica. Michigan State University Graduate School also supplied additional funding. I greatly appreciated that my advisor, Lina Patino, offered guidance throughout this process, along with interest and faith in my project. My committee members, Tom Vogel and Duncan Sibley, provided input and assistance in meeting deadlines. Thanks also to the department office and library staff for your help. Sampling in Costa Rica, would not have went smoothly without Guillermo Alvarado. Kennet Flores also provided samples, maps, and information on my sample locations. Thanks to Chad Deering and Dave Szymanski for the laughs and the muscle behind the sledgehammer in Costa Rica. Thanks also to Ela Viray for passing on data from Nicaragua.

I also appreciate the support of my fellow graduate students, friends, and family. Thanks to Hillery and Ryan, Karen Tefend, Amy Lansdale, Leah Piwinski, Mike Kramer, Michelle Vit, Brent & Miranda Lucyk, Tim Place, Robin Rumpf and my Mom.

TABLE OF CONTENTS

LIST OF TABLES.....	v
LIST OF FIGURES	vi
INTRODUCTION.....	1
Background.....	1
Sample Locations.....	6
METHODS	9
Sampling Methods	9
Sample Preparation.....	10
Analytical Techniques	10
RESULTS.....	12
Petrography	12
Alteration.....	29
Geochemistry	33
DISCUSSION	55
Mantle Source.....	55
Slab Signal.....	59
Speculations on Subducted Sediment.....	64
CONCLUSIONS	69
APPENDICES.....	72
Appendix A: Petrographic descriptions of altered samples	73
Appendix B: Minerals present in thin sections	82
Appendix C: Anomalous slab signal (Ce/Pb)	85
REFERENCES	95

LIST OF TABLES

Table 1. Petrographic descriptions of lava samples.....	13
Table 2. Major and trace element geochemistry from the primitive arc volcaniclastic lavas. Samples not collected in the 2004 field season originated from (#) Kennet Flores and location is in the Costa Rican coordinate system, (+) Patino and others (2004), and (=) T.A. Vogel. .	34
Table 3. Range of select trace element ratios for primitive arc lavas.	56
Table 4. Minerals present in thin section.....	83

LIST OF FIGURES

- Figure 1.** From the Late Oligocene-Early Miocene to present, the modern Central American volcanic arc results from the Cocos Plate beneath the Caribbean Plate. Figure modified from Feingenson et al., 2004.2
- Figure 2.** A reconstruction of the Central American arc during the Paleocene and Eocene. The Farallon Plate is subducting beneath the Caribbean Plate. Figure modified from Hauff et al., 2000.....3
- Figure 3.** A map of the primitive arc sample locations in Costa Rica. Sample locations are as follows: 1. Punta Samara, 2. Isla Paloma, 3. Quebrada Buenaventura, and 4. Playa Soley.7
- Figure 4.** Photos of volcaniclasts from the primitive arc located at8
- Figure 5.** Photomicrograph of a lava sample, 040709-15, from Quebrada Buenaventura, in plane polarized light (top) and crossed polarized light (bottom). Plagioclase, pyroxene, and opaques form the phenocryst assemblage in lava samples from Punta Samara, Isla Paloma, and Quebrada Buenaventura, and 2 lava samples from Playa Soley (040710-16 and 040709-19). Plag is plagioclase, Pyx is pyroxene, Opq is opaque, and Cal is calcite.25
- Figure 6.** Photomicrograph of lava sample, 040709-2, from Quebrada Buenaventura, in plane polarized light (top), and cross polarized light (bottom). Reaction rims are present on some pyroxene grains.26
- Figure 7.** Photomicrograph of a lava sample, PA10, from Punta Samara, in plane polarized light (top) and crossed polarized light (bottom). Complete or partial replacement of grains by secondary products was present in some samples. Plag is plagioclase, Opq is opaque, Cal is calcite, Chl is chlorite, and repl is completely replaced grain.27
- Figure 8.** Photomicrograph of a fiamme sample, 031024-4a, from Playa Soley, in plane polarized light (top) and crossed polarized light (bottom). Anhedral feldspar and quartz form the phenocryst assemblage in

fiamme samples from Playa Soley, and opaques appear to be secondary. Plag is plagioclase, Repl is completely replaced grain. ...28

- Figure 9.** The majority of the modern arc volcanic samples have Weathering Index of Parker (WIP) values > 60. Primitive arc samples with WIP values < 60 (open primitive arc symbols) were not included in the geochemical portion of this study.31
- Figure 10.** Pumice 031024-4a, 4b, 4e, and 4h from Playa Soley have unusual REE patterns. These samples were not included in the geochemical portion of this study.32
- Figure 11.** Total alkalis versus SiO₂ classification diagram of Le Bas et al. (1986) of the primitive arc volcanoclasts.49
- Figure 12.** Major element variation versus SiO₂ (wt%) amongst the primitive arc lava samples50
- Figure 13.** Trace element concentrations (ppm) versus SiO₂ (wt%) for the primitive arc lava samples.51
- Figure 14.** The spider diagram, normalized to the primitive mantle after Sun and McDonough (1989), illustrates that the primitive arc lavas samples are enriched in LILE relative to HFSE, characteristic of volcanics originated from subduction zone magmatism.53
- Figure 15.** REE trend for the lava samples from the primitive arc are relatively similar to each other. Normalized to chondrite after Sun and McDonough (1989).54
- Figure 16.** Volcanics with higher Zr/Nb ratios indicate a more depleted mantle source. Increasing Ba/La ratios indicate greater slab contribution to the lavas. DM and EM compositions are N-MORB and OIB, respectively, from Sun and McDonough, 1989.58
- Figure 17.** The Zr/Nb (A) and Ba/La ratios (B) of the lava samples are not correlated with SiO₂ (wt%).60

- Figure 18.** The Ba/La ratios from the volcanics from the primitive arc (A) show a correlation with the La/Yb ratio, similar to the modern arc volcanics (B).62
- Figure 19 .** The Ba/Th variation for the primitive arc also decreases with an increase in La/Yb ratio (A). The primitive arc lava samples have Ba/Th ratios most similar to Miocene and modern western Nicaraguan volcanics (B).66
- Figure 20.** The primitive arc lava samples have U/Th ratios similar to those from Miocene Nicaragua and modern Costa Rica.67
- Figure 21.** Comparison of the primitive arc in Costa Rica (A) to the modern arc in Costa Rica (B) and western Nicaragua (C). Diagram after Carr et al., 1990.71
- Figure 22.** Some lava samples from the primitive arc have high Ce/Pb ratios and high Ba/La ratios (>50). Samples from the primitive arc with Ce/Pb ratios >14 are shown as open symbols. OIB and MORB are from Sun and McDonough, 1989.87
- Figure 23.** The lava samples with high Ce/Pb ratios from the primitive arc (open symbols) are due to low Pb concentrations in the samples. MORB and OIB are from Sun and McDonough, 1989.88
- Figure 24.** The low-Pb lava samples have the characteristics of arc related magmatism. OIB and MORB are from Sun and McDonough, 1989.91
- Figure 25.** Selected elements versus Pb. Notice that the low-Pb samples (open symbols) also have low K₂O (wt%), Rb, Th, and U (ppm) compared to other primitive arc lava samples. However, the low-Pb samples do not have the lowest concentrations of Ce and Ba (ppm).94

Introduction

Background

The modern Central American volcanic arc is located along the western portion of the Caribbean Plate (Figure 1). From the Late Oligocene-Early Miocene to present, the arc is the product of the subduction of the oceanic Cocos Plate underneath the Caribbean Plate (Hey, 1977). However, there is evidence of subduction related volcanism prior to the Oligocene along the western portion of the Caribbean Plate (Bourgois et al., 1984; Meschede et al., 1988; Maury et al., 1995; Hauff et al., 2000; Lissinna et al., 2002). The earlier arc was the result of the Farallon Plate subducting beneath the Caribbean Plate (Pindell and Barrett, 1990; Hauff et al., 2000; Hoernle et al., 2002) (Figure 2). The Farallon Plate broke into the southern Cocos and Nazca plates and the northern Juan de Fuca Plate, at approximately 22.7 Ma (Hey, 1977; Barckhausen et al., 2001).

The earliest appearance of subduction related volcanism in southern Central America is found in formations from the Aptian to the Eocene (Bourgois et al., 1984; Tournon, 1984; Calvo and Boltz, 1994; Hauff et al., 2000; Hoernle et al., 2002; Lissinna et al., 2002). In the Santa Elena peninsula in Costa Rica, Hauff et al. (2000) reported arc related rocks dated between 124 and 109 Ma. Along the Pacific coast in Costa Rica, andesitic cobbles are found in Campanian to Paleocene turbidite deposits (Kuijpers, 1979; Lew, 1983). Manifestations of the ancient arc are also found in other areas of Central America. Cenomanian to Eocene volcanoclastic sediments are found on the Nicaraguan Trough (Weyl, 1980). Weyl (1980) suggests that these originated from Cretaceous to Tertiary

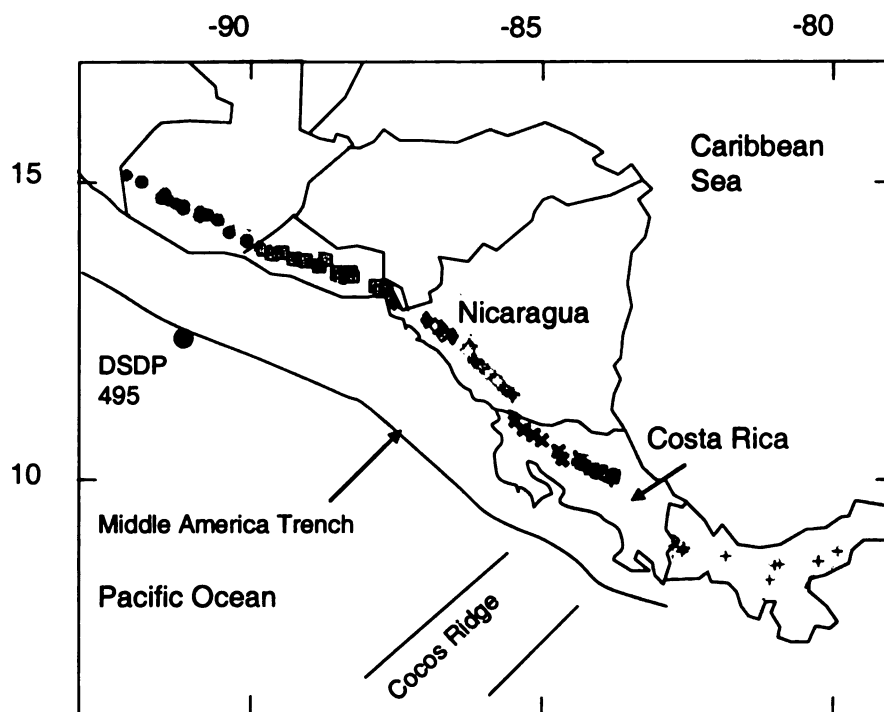


Figure 1. From the Late Oligocene-Early Miocene to present, the modern Central American volcanic arc results from the subduction of the Cocos Plate beneath the Caribbean Plate. Figure modified from Feigenson et al., 2004.

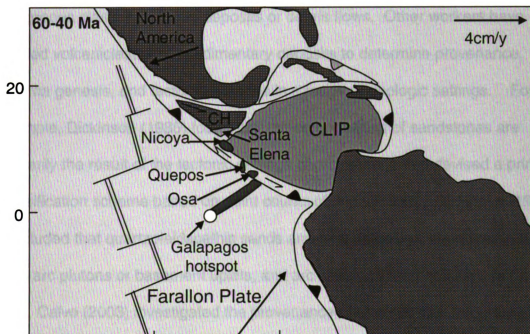


Figure 2. A reconstruction of the Central American arc during the Paleocene and Eocene. The Farallon Plate is subducting beneath the Caribbean Plate. Figure modified from Hauff et al., 2000. CH is the Chortis Block, CLIP is Caribbean Large Igneous Province.

subduction, which produced volcanism in southeastern Central America. In western Panama, on Coiba Island, Lissinna et al. (2002) indicate that subduction-related calc-alkaline lavas (48.8 to 60.89 Ma) are present. Maury et al. (1995) utilized petrography and geochemistry to determine that Late Eocene volcaniclasts located in streambeds from the Turia-Chucunaque Basin in eastern Panama were related to an early volcanic arc.

In Costa Rica, the most common manifestations from the earlier arc occur as igneous clasts in turbidite deposits or debris flows. Other workers have studied volcaniclasts from sedimentary deposits to determine provenance, magma genesis, and tectonic histories in a range of geologic settings. For example, Dickinson (1985) found that the compositions of sandstones are primarily the result of the tectonic settings of provenance and devised a primary classification scheme based on point counts of thin sections. Dickinson (1985) concluded that quartzofeldspathic sands and feldspatholithic sands originated from arc plutons or basement uplifts, and arc volcanics, respectively. In Costa Rica, Calvo (2003) investigated the provenance of plutonic rock fragments in sandstones from El Viejo and Rivas Formations. Calvo (2003) used point counts of thin sections to conclude that the sandstones, underlain by the Nicoya Complex, originated partially from the erosion of this complex.

In addition, studies based on the geochemistry of volcaniclasts have also been used to make geologic interpretations. For example, Saito (1998) used major and trace element geochemistry of cuttings from drill cores, which included volcaniclastic sediments and turbidites, to determine provenance and

paleoenvironmental changes in the East Greenland Margin. Using Nd-Pb isotopic compositions of volcanoclastic sandstones preserved in turbidite deposits, Gill et al. (1994) inferred the temporal variation in sources of volcanics from the Izu-Bonin arc. Gill et al. (1994) also resolved changes in the arc, such as back arc basin formation, from variations in major and trace element geochemistry of volcanoclastic material. Schott and Johnson (1998) utilized the geochemistry of igneous conglomerate clasts from the Cretaceous Gualala basin in California to infer an arc related origin and paleotectonics of the region. Lytwyn et al. (2001) investigated the geochemistry of the Late Cretaceous turbidite deposits to infer the origin of the Sumba region in Indonesia, and found a close proximity to an intra-oceanic island arc. In a modern example, Ballance (1991) describes that debris and gravity flows are responsible delivering volcanoclastic debris and turbidites to different areas of the Tonga Trench slope. The author states that several stages of transport may be possible before volcanoclasts arrive at the deep trench slope.

Similar to the above studies, this study characterizes the petrography and geochemistry of volcanoclasts from three sample locations, along with more detailed information on an area described by Patino et al. (2003) in Costa Rica to infer subduction parameters. The volcanoclasts range in age from Late Cretaceous to Eocene. In this thesis, these volcanics are referred to as expressions of the “primitive arc”, based on the temporal difference with the modern arc in Central America. Geochemical compositions of the primitive arc lavas are then compared to samples from the volcanic front from the modern arc,

concentrating on the Costa Rican and Nicaraguan segments, to determine the subduction parameters for the primitive arc.

Sample Locations

Sample locations include Isla Paloma, Quebrada Buenaventura, and Playa Soley which are located in Costa Rica. The outcrop at Punta Samara, Costa Rica, studied by Patino et al. (2004), will also be included. Figure 3 shows a map of sample locations in Costa Rica.

Patino et al. (2004) collected volcanic cobbles (Figure 4) from a turbidite deposit located in the northern portion of Punta Samara (coordinates not recorded). Twelve lava clasts are included in this study from Punta Samara. According to Baumgartner et al. (1984), the volcaniclasts from Punta Samara were deposited during the Upper Maastrichtian and the Lower-Middle Paleocene. The mechanical weathering of lava flows most likely created the volcaniclasts. The volcanic cobbles were part of high density submarine flows from an unstable shallow marine platform (Baumgartner et al., 1984).

Isla Paloma is located to the west of Isla Chira in the Gulf of Nicoya, at approximately 10.11° N and 85.20° W. According to Flores (2003), the outcrop at Isla Paloma is part of the Cerco de Pierda Member of the Descartes Formation. The Descartes Formation (Middle to Upper Paleocene) is a conglomerate that contains angular to rounded clasts, and it is associated with a carbonate platform (Rivier, 1985; Flores, 2003). Volcaniclasts within the Formation range from basaltic to andesitic (Flores, 2003). The volcaniclasts in the Cerco de Pierda Member are mostly andesitic, but basaltic compositions are

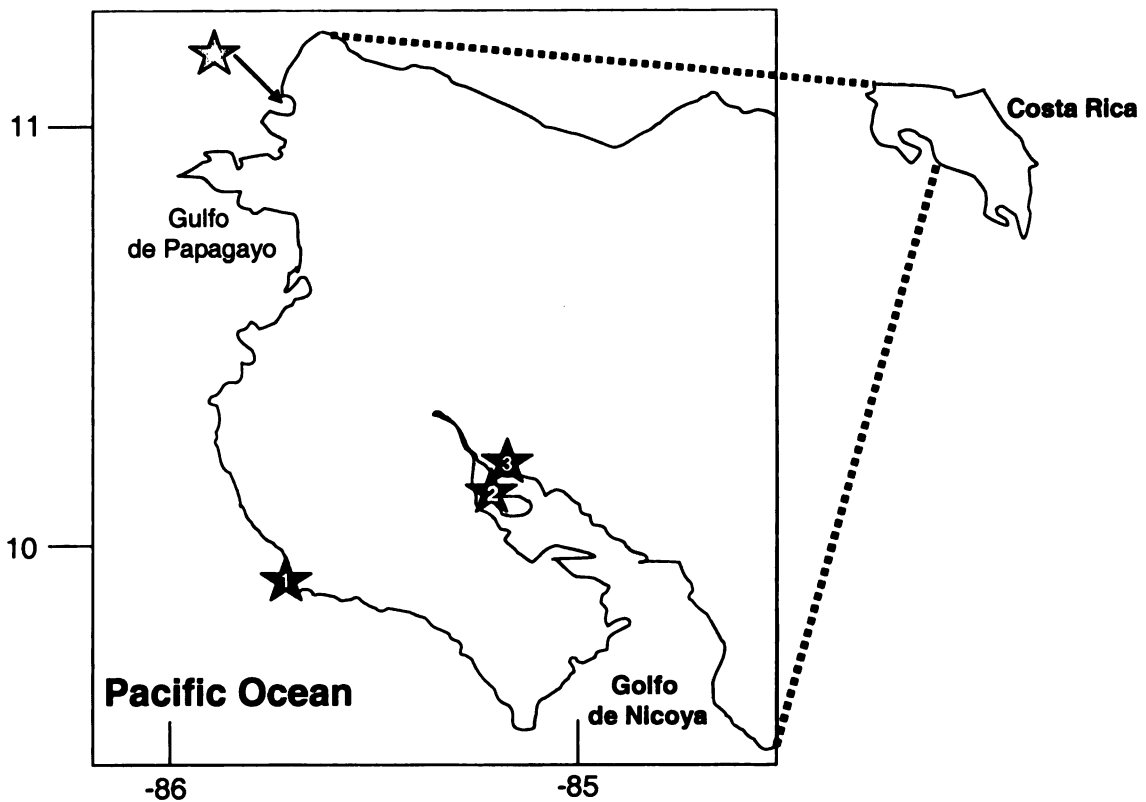


Figure 3. A map of the primitive arc sample locations in Costa Rica. Sample locations are as follows: 1. Punta Samara, 2. Isla Paloma, 3. Quebrada Buenaventura, and 4. Play Soley.

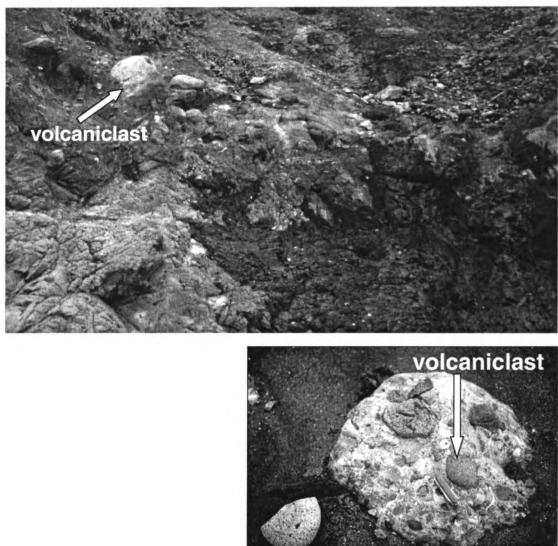


Figure 4. Photos of volcaniclasts from the primitive arc located at Punta Samara.

also present (Flores, 2003). Thirteen lava clasts were included in this study from Isla Paloma.

Samples were taken along a creek, Quebrada Buenaventura, which is located at approximately 10.65° N and 85.42° W. Samples from Quebrada Buenaventura are also from the Cerco de Pierda Member of the Descartes Formation (Flores, 2003). The igneous clasts collected at this location included 12 lavas samples.

Playa Soley is located 11.04° N and 85.67° W. At this location both lava and ignimbrite clasts occurred in a turbidite deposit or debris flow. The samples from Playa Soley are inferred to be Eocene in age (Alvarado, personal communication, 2003). Eleven ignimbrite and six lava samples were collected from this location. Two lava clasts were collected by Kennet Flores just east of Playa Soley at Playa Rajada. The samples from Playa Rajada are from the Descartes Formation.

Methods

Sampling Methods

This study includes sixty samples, which consists of 14 ignimbrite and 46 lava samples. The majority of these hand samples were collected during the 2004 field season. Nine ignimbrite samples were previously collected during October 2003 by T.A. Vogel (Michigan State University). Five lava samples were provided by Kennet Flores (Universidad de Costa Rica). Twelve of the samples were collected during the 1999 field season by Patino et al.,(2004).

Geochemical analyses of ignimbrites were performed on fiamme fragments from the collected hand samples. When whole fiamme fragments could not be obtained from the ignimbrite hand samples, only thin sections were prepared. Geochemical analyses were performed on all lava samples, except for one, which was obviously altered and collected solely for petrographic analysis.

Sample Preparation

Hand samples were cut to extract whole fiamme fragments or the center and, presumably the freshest portion, of the ignimbrite and lava samples, respectively. The extracted portions were submerged in a sonic bath for approximately 20 minutes and dried. The samples were then disaggregated using a chipmunk and ground into a fine rock powder using a ceramic flat plate grinder.

Fused glass disks were made for each sample using a mixture of 3.0 g of rock powder, 9.0 g of a low temperature flux, lithium tetraborate ($\text{Li}_2\text{B}_4\text{O}_7$), and 0.5 g of an oxidizer, ammonium nitrate (NH_4NO_3). The mixture was melted in platinum crucibles at $1,000^\circ\text{C}$ over an oxidizing flame for 20 to 30 minutes while stirred on an orbital mixing stage. The melted samples were then poured into platinum molds to form glass disks.

Analytical Techniques

Major element chemistry and select trace element chemistry were obtained by X-ray fluorescence (XRF), and additional trace elements were

obtained through laser ablation inductively coupled plasma mass spectrometry (LA ICP-MS). For XRF, analyses were performed on the glass disks using a Rigaku S/Max or a Bruker S4Pioneer X-Ray fluorescent spectrograph at Michigan State University. Major element XRF data was processed using a fundamental parameter data reduction method (Criss, 1980), using XRFWIN or SPECTRA^{PLUS} software for the Rigaku S/Max and Bruker S4Pioneer, respectively. XRF trace element data were calculated using standard linear regression.

Trace element analyses were performed at Michigan State University using a Cetac LSX200+ laser ablation system coupled with a Micromass Platform ICP Mass Spectrometer. A 266 nm UV laser is used in this system. For most samples, the laser was fired at a frequency of 10 Hz. A preablation scan rate of 150 $\mu\text{m}/\text{sec}$ was used with a spot size of 250 μm . The ablation parameters were a scan rate of 10 $\mu\text{m}/\text{sec}$, a spot size of 200 μm , and a defocus of 50 μm . For samples that had a high SiO_2 content, the laser was fired at a frequency of 20 Hz. Preablation conditions for high SiO_2 samples were a scan rate of 50 $\mu\text{m}/\text{sec}$, a spot size of 250 μm , and a defocus of 100 μm . The ablation conditions for these samples were a scan rate of 10 $\mu\text{m}/\text{sec}$, a spot size of 200 μm , and a defocus of 200 μm . Strontium from the XRF analyses was used as the internal standard to calculate LA ICP-MS results. A linear regression method using USGS and Japanese rock standards determined the trace element concentrations in the samples using MassLynx Software. The background

values are subtracted from the samples and standards prior to calculation of concentrations.

RESULTS

Petrography and Mineralogy

Only the least altered samples were chosen for the study. Detailed petrographic descriptions are included in Table 1 for samples that were included in the geochemical portion of the study. Appendix A contains petrographic descriptions of samples that were not included in the geochemical portion of the study. Appendix B contains a list of the minerals present in each sample.

Petrographic analyses were performed on sixty thin sections. Grains 0.5 mm and greater were considered phenocrysts. The lava clasts from the primitive arc at Punta Samara, Isla Paloma, Quebrada Buenaventura, and two from Playa Soley do not vary in mineralogy among sample locations. These lavas are comprised of 35 to 65% phenocrysts euhedral to subhedral phenocrysts of plagioclase and pyroxene, and subhedral to anhedral opaques (Figure 5). Sericite was present on the majority of the plagioclase phenocrysts. Many samples contained reaction rims on the pyroxene phenocrysts (Figure 6). The partial or complete replacement of phenocrysts by secondary minerals, including calcite and chlorite occurred in most sections (Figure 7). The groundmass consists of microphenocrysts and alteration products.

The remaining lava samples from Playa Soley have a small percentage of phenocrysts of anhedral feldspar, opaques, and quartz. The

Table 1. Petrographic description of lava samples.

Sample	Description
PA5	<p>Sample PA5 is a dacite from Punta Samara. Phenocrysts comprise 55% of the sample. Forty percent of the phenocrysts are subhedral plagioclase and are up to 2.4 mm in length. Phenocrysts of plagioclase exhibit sericite and some are altered to chlorite. Subhedral pyroxene phenocrysts are up to in 0.75 mm in size and comprise 5% of the sample. Reaction rims are present on some of the pyroxene phenocrysts. Opaques are included within the pyroxene grains. Less than 1% of the grains are replaced by opaques and alteration products. Anhedral opaques are up to 0.5 mm in size and comprise 5% of the sample. Larger opaques appear to be secondary. The groundmass comprises 45% of the sample and consists of the phenocrysts assemblage, cryptocrystalline material, opaques, and veins of alteration products and possibly quartz. Cryptocrystalline. The quartz veins may explain the difference between the chemistry and mineral assemblage.</p>
PA6	<p>Sample PA6 is a basaltic andesite from Punta Samara. The phenocrysts comprise 45% of the sample. Subhedral plagioclase phenocrysts comprise 35% of the sample and are up to 2 mm in size. Plagioclase phenocrysts exhibit sericite and partial alteration to chlorite. Five percent of the sample is comprised subhedral pyroxene grains are up to 4 mm in size and most are broken. Anhedral opaques comprise 5% of the sample and are up to 1 mm in size. Some opaques may be secondary. The groundmass comprises 55% of the sample. The groundmass consists of the phenocryst assemblage and previously mentioned alteration products. Calcite is also present in 5% of the groundmass.</p>
PA9	<p>Sample PA9 is a basaltic andesite from Punta Samara. Phenocrysts comprise 55% of the section. Forty percent of the phenocrysts are subhedral plagioclase that are up to 2 mm in size. Plagioclase phenocrysts display sericite and are partially altered to chlorite. Five percent of the phenocrysts consist of subhedral pyroxene, and are up to 3.5 mm in size. The majority of the phenocrysts are broken and reddish brown alteration crosses the crystals. Approximately 5% of the phenocrysts are completely altered to calcite and less than 1% to chlorite. Anhedral opaques comprise 5% of the phenocrysts and are up to 1 mm in size. Some opaques may be secondary. The groundmass comprises 45% of the sample. The groundmass consists of the phenocryst assemblage and alteration products in approximately the same proportion.</p>

Table 1. (continued)

Sample	Description
PA11	Sample PA11 is an andesite from Punta Samara. The sample consists of 50% phenocrysts. Forty percent of the phenocrysts are subhedral plagioclase that are up to 3.5 mm in size. Sericite is present on the plagioclase. Ten percent of the phenocrysts are subhedral pyroxene that are up to 3.5 mm in size. The majority of the pyroxene phenocrysts are broken. Opaques are included in the phenocrysts. Secondary opaques that have reaction rims of reddish brown material are also present near phenocrysts and are up to 1 mm in size. Less than 1% of the phenocrysts have been completely replaced by calcite. The sample contains 50% groundmass that is approximately 35% plagioclase microlites and less than 1% microphenocrysts of pyroxene. Opaques comprise approximately 15% of the groundmass. Fissures of calcite are present in less than 1% of the section.
PA12	Sample PA12 is an andesite from Punta Samara. The section is composed of 45% phenocrysts. Thirty-five percent of the phenocrysts are subhedral plagioclase that are up to 2.25 mm in length. Subhedral pyroxene are present in 10% of the sample, and the grains are up to 3 mm in size. Alteration to chlorite is present on a small percentage of phenocrysts. Opaques are included in pyroxene phenocrysts. Anhedral opaques are up to 1 mm in size and display reaction rims. Less than 1% of the phenocrysts are completely replaced by calcite. The groundmass comprises 55% of the section. The groundmass consists of 40% microphenocrysts is the same proportion as the phenocryst assemblage and included 15% opaques.
PA13	Sample PA13 is a basaltic andesite from Punta Samara. The section is comprised of 65% phenocrysts. Fifty-five percent of the phenocrysts are subhedral plagioclase that are up to 2 mm in size. Sericite is present on plagioclase grains. Five percent of the sample is subhedral pyroxene phenocrysts. Altered phenocrysts are present in 5% of the sample including phenocrysts that have reaction rims of opaques and those that have been completely replaced by calcite. Partial alteration to chlorite also occurs on the phenocrysts. The groundmass comprises 35% of the section. The groundmass is comprised of microphenocrysts and alteration products in the same percentage as previously described.

Table 1. (continued)

Sample	Description
PA14	Sample PA14 is a basaltic andesite from Punta Samara. The sample consists of 45% phenocrysts. Subhedral plagioclase phenocrysts comprise 35% of the sample. Sericite is present on the plagioclase. Alteration to chlorite is also present on the phenocrysts. Ten percent of the phenocrysts are subhedral pyroxene that are up to 1 mm in size. Anhedral opaques are included in the pyroxene, and are up to 0.5 mm in size. Calcite replaced less than 1% of the phenocrysts. The groundmass is 55% of the section. The groundmass consists of microphenocrysts in the same proportion as the phenocrysts and opaques. The groundmass also contains less than 1% calcite.
PA15	Sample PA15 is a basaltic andesite from Punta Samara. The sample consists of 35% phenocrysts. Twenty-five percent of the phenocrysts are subhedral plagioclase that are up to 2 mm in size. Plagioclase phenocrysts display little sericite. Subhedral pyroxene phenocrysts are up to 2 mm in size. Reaction rims are present on most pyroxene and secondary opaques are also present near the grains. A small amount of alteration to chlorite is present on some phenocrysts. The groundmass is comprised of a similar mineralogy as the phenocryst assemblage.
PA18	Sample PA18 is a basaltic andesite from Punta Samara. The phenocrysts comprise approximately 35% of the sample. Subhedral plagioclase phenocrysts contribute to 35% of the section, and are up to 1.5 mm in length. Subhedral pyroxene are up to 1 mm in length. Approximately 1% of the phenocrysts have been completely altered to calcite. Alteration to chlorite is also present on phenocrysts. The groundmass consists of 30% microphenocrysts, 20% opaques, 10% calcite and 5% chlorite.

Table 1. (continued)

Sample	Description
040709-15	Sample 040709-15 is an andesite from Isla Paloma. Fifty-five percent of the sample is composed of phenocrysts. Forty-five percent of the sample is comprised of subhedral plagioclase phenocrysts are up to 1.6 mm in length. Approximately 1% of the plagioclase grains have been completely replaced with calcite. Sericite is present on the plagioclase grains as well as, partial alteration to calcite and chlorite. The subhedral pyroxene phenocrysts comprise 10% of the section and are up to 1.5 mm in size. Reaction rims of opaques are present around the majority of the pyroxene phenocrysts. Less than 1% of what appears to have been pyroxene phenocrysts are replaced with opaques and a reddish brown material. Clots of smaller plagioclase, pyroxene, and replaced grains occur in the section. Five percent of the section is anhedral opaques that are up to 1.25 mm in size. The groundmass comprises 45% of the sample and contains 35% cryptocrystalline material and 10% opaques.
040709-16	Sample 040709-16 is a dacite from Isla Paloma. Fifty-five percent of the sample is composed of phenocrysts. Subhedral plagioclase phenocrysts are up to 3.5 mm in length and display sericite, alteration to calcite and chlorite. Plagioclase phenocrysts comprise 40% of the sample. Less than 1% of the plagioclase phenocrysts have been completely replaced by calcite. Fifteen percent of the sample is comprised of subhedral pyroxene phenocrysts that are up to 2.5 mm in size. Less than 1% of what may have been pyroxene phenocrysts has reaction rims of opaques and appears to be replaced with a reddish brown material. Anhedral opaques comprise 5% of the phenocrysts and are up to 1 mm in size. Clots of smaller plagioclase, pyroxene, opaques, and replaced grains occur in the section. The cryptocrystalline groundmass, which composes 40% of the sample, appears to be 30% cryptocrystalline material and 10% opaques. Lines of reddish brown alteration cross the section in PPL.

Table 1. (continued)

Sample	Description
040709-17	Sample 040709-17 is a basaltic andesite from Isla Paloma. Sixty-five percent of the sample is composed of phenocrysts. Fifty percent of the sample is subhedral plagioclase phenocrysts that are up to 2.6 mm in length. Sericite is present on the plagioclase. Fifteen percent of the sample is composed of pyroxene phenocrysts and are up to 1.3 mm. The majority of pyroxene phenocrysts have reaction rims of opaques and are almost completely altered to chlorite. The groundmass comprises 30% of the sample consisting of 20% cryptocrystalline material, 10% opaques, and 5% chlorite.
040709-18	Sample 040709-18 is a basaltic andesite from Isla Paloma. Phenocrysts comprise 65% of the sample. Forty-five percent are plagioclase phenocrysts up to 2.5 mm in size. Sericite is present on the plagioclase, along with alteration to chlorite. Approximately 5% of the grains are completely altered to chlorite. Subhedral pyroxene phenocrysts are up to 1.5 mm in size and comprise 10% of the sample. Opaques are included within the pyroxene. Approximately 1% of the phenocrysts are anhedral opaques that are up to 1 mm. Forty percent of the sample is comprised of the groundmass which includes 30% cryptocrystalline material and 10% opaques.
040709-20	Sample 040709-20 is an andesite from Isla Paloma. The sample is comprised of 40% phenocrysts. Thirty percent are subhedral plagioclase phenocrysts that are up to 1.5 mm in length. Sericite and alteration to chlorite occurs on the plagioclase grains. Ten percent of the sample is comprised of subhedral pyroxene phenocrysts are up to 1 mm. Opaques are included with pyroxene grains. The groundmass comprises 60% of the sample and includes 25% cryptocrystalline material, 10% chlorite, 15% plagioclase microlites, and 10% opaques.

Table 1. (continued)

Sample	Description
040709-21	Sample 040709-21 is a basaltic trachyandesite from Isla Paloma. The phenocrysts comprise 60% of the section. Forty percent of the phenocrysts are comprised of subhedral plagioclase phenocrysts are up to 2 mm in size. Plagioclase grains display sericite and alteration to chlorite. Euhedral pyroxene phenocrysts comprise 20% of the section and are up to 2.5 mm in size. Opaques are included in pyroxene grains. The groundmass comprises 40% of the section. The groundmass is comprised of 15% phenocryst assemblage, 10% opaques, 10% cryptocrystalline material, and 5% chlorite. A vein runs through the section calcite.
040709-22	Sample 040709-22 is a basaltic andesite from Isla Paloma. The phenocrysts comprise 55% of the sample. Subhedral plagioclase phenocrysts compose 55% of the sample and are up to 2 mm in size. Sericite and partial alteration to chlorite and calcite is present on the plagioclase phenocrysts. Approximately 2% of the phenocrysts have been completely replaced by calcite. Subhedral pyroxene phenocrysts up to 0.6 mm in size comprise less than 1% of the sample. Secondary opaques are included in broken and replaced phenocrysts. Forty-five percent of the sample is the groundmass. Twenty percent of the groundmass is comprised of the phenocryst assemblage and alteration products, 15% cryptocrystalline material, and 10% opaques are also present.
040709-24	Sample 040709-24 is an andesite from Isla Paloma. The sample is comprised of 40% phenocrysts. Subhedral plagioclase phenocrysts compose 20% of the section and are up to 2.8 mm in size. Sericite is present on plagioclase grains. Chlorite appears along mineral fissures. Subhedral pyroxene phenocrysts are up to 1.5 mm in size and are present in 10% of the section. Ten percent of the phenocrysts appear to be secondary amphibole. Secondary opaques are up to 1 mm in size and occur near pyroxene grains and grains that appear to have altered to amphibole. The groundmass is comprised of 35% cryptocrystalline material possibly from the phenocryst assemblage and alteration products and 25% opaques.

Table 1. (continued)

Sample	Description
040709-25	Sample 040709-25 is a basaltic andesite from Isla Paloma. The sample contains 50% phenocrysts. Forty percent of the phenocrysts are comprised of subhedral plagioclase are up to 2.3 mm in size. The plagioclase phenocrysts exhibit sericite alteration. Ten percent of the phenocrysts are composed of subhedral pyroxene are up to 2.5 mm in size and account for 10% of the section. Both plagioclase and pyroxene contain inclusions of opaques. Reaction rims are present along a few pyroxene grains and less than 1% of the pyroxene are almost completely replaced by secondary opaques. Alteration to chlorite is present on phenocrysts. The groundmass consists of the 40% microphenocrysts as in the same proportion as the phenocryst assemblage and 10% opaques.
14-11-1201	Sample 14-11-1201 is an andesite from Isla Paloma. The sample consists of 40% phenocrysts. Subhedral plagioclase phenocrysts are up to 2 mm in length. Plagioclase phenocrysts display sericite and alteration to calcite and chlorite. Subhedral pyroxene phenocrysts are up to 1.5 mm in size and have reaction rims of a reddish brown material and alteration to chlorite. Opaques are up to 0.5 mm in size and comprise 15 % of the sample. The groundmass is 60% of the sample. The groundmass consists of microphenocrysts and alteration products.
13-11-1201	Sample 13-11-1201 is an andesite from Isla Paloma. The phenocrysts comprise 35% of the sample. Twenty-five percent of the phenocrysts are subhedral feldspar phenocrysts that are up to 2.8 mm. Plagioclases exhibit sericite and alteration to chlorite. Subhedral pyroxene phenocrysts are up to 2.8 mm in size. Opaques are included in pyroxene grains. Reaction rims are present around several phenocrysts. The groundmass comprises 65% of the sample. The groundmass consists of 35% of the phenocryst assemblage. Secondary opaques comprise 15% of the section and are up to 0.8 mm in size. The remaining portion of the section appears to be alteration products including calcite and chlorite. A calcite vein runs across the section.

Table 1. (continued)

Sample	Description
040709-1	Sample 040709-1 is a basaltic trachyandesite from Quebrada Buenaventura. The sample is composed of 40% phenocrysts. Phenocrysts consist of plagioclase, pyroxene, and replaced phenocrysts. Thirty-five percent of the phenocrysts are plagioclase that range up to 2.5 mm. Plagioclase phenocrysts occasionally have inclusions of pyroxene. Plagioclase phenocrysts display sericite. Some plagioclase phenocrysts have been partially altered to secondary products, mostly calcite and chlorite. Other phenocrysts, approximately 5% of the sample, have been completely replaced by a combination of secondary products including opaques, chlorite, and calcite. Some of these may have been olivine phenocrysts. Less than 1% of the sample is composed of euhedral pyroxene phenocrysts that display exsolution lamellae and are up to 0.8 mm. Opaque minerals constitute <1% of the phenocrysts and are up to 0.5 mm. The sample is composed of 60% groundmass that contains 25% opaques (probably secondary), 15% cryptocrystalline material, 10% plagioclase microlites, 5% chlorite, and 5% calcite. Fissures of alteration products cut across areas of the section.
040709-2	Sample 040709-2 is an andesite from Quebrada Buenaventura. This sample contains 65% of generally fine grained phenocrysts. Forty-five percent are subhedral plagioclase phenocrysts that are up to 1.25 mm long, with the majority near 1 mm long, and exhibit sericite. The plagioclase phenocrysts appear to have reaction rims along some edges (looks like resorbing). Ten percent of the sample is subhedral pyroxene up to 1 mm in length. There are reaction rims around pyroxene grains. Opaques are included in the plagioclase and pyroxene grains. Five percent of the phenocrysts are completely replaced with calcite and/or chlorite and also have reddish brown alteration. The groundmass comprises 35% of the sample and includes 10% of the phenocryst assemblage, 5% cryptocrystalline material, 5% opaques, 5% chlorite, 5% calcite, and <1%reddish brown alteration.

Table 1. (continued)

Sample	Description
040709-3	Sample 040709-3 is a basaltic trachyandesite from Quebrada Buenaventura. This sample is composed of 65% phenocrysts. This sample is composed of 60 % subhedral plagioclase up to 2.3 mm in length, along with fragments of grains that may have been larger. Sericite is present in the plagioclase grains. Five percent of the sample is composed of subhedral pyroxene phenocrysts that are up to 1.3 mm long. Opaques that are probably secondary are up to 0.5 mm. Reaction rims are present around pyroxene grains and an abundance of opaques. Calcite and chlorite occur on grains and calcite has replaced <1% of the grains. The sample is composed of 35% groundmass, which includes 20% smaller crystals of the phenocryst assemblage, 5% secondary opaques, 5% calcite, and 5% chlorite.
040709-5	Sample 040709-5 is an andesite from Quebrada Buenaventura. Forty percent of the sample is composed of phenocrysts. Subhedral plagioclase phenocrysts are up to 1.25 mm in length, and comprise 30% of the sample. Sericite is present on the plagioclase grains. Fifteen percent of the sample is composed of subhedral pyroxene phenocrysts that are up to 0.625 mm in size. Reaction rims of opaques and reddish brown material surround the pyroxene phenocrysts. The opaques appear to be secondary and comprise. The groundmass is composed of microphenocrysts of 40% plagioclase, 15% opaques, 5% cryptocrystalline material and <1% calcite and chlorite.

Table 1. (continued)

Sample	Description
040709-6	<p>This sample is a trachyandesite from Quebrada Buenaventura and is composed of 35% phenocrysts. Twenty-five percent of the phenocrysts are subhedral plagioclase that range from 0.75 to 5 mm in length. Sericite, along with alteration to calcite and chlorite is present in the plagioclase phenocrysts. Euhedral pyroxene phenocrysts range from 0.375 to 1 mm in size and comprise 5 % of the section. Approximately 5% of the phenocrysts are completely replaced calcite and chlorite replaced grains. Phenocrysts appear to be partially and completely replaced by calcite and chlorite. Less than 1% of the sample is composed of anhedral opaque phenocrysts, which appear to be secondary and occur near pyroxene phenocrysts. These are up to 0.5 mm in size. The groundmass comprises 65% of the sample. Veins of predominately calcite traverse the section. Secondary opaques are present. The groundmass is composed of 20% cryptocrystalline material, 20% is possibly remnants of plagioclase microlites, 10% opaques, and 10% calcite and 5% chlorite. Reddish brown alteration is less than 1% of the sample.</p>
040709-9	<p>This is a basaltic trachyandesite from Quebrada Buenaventura. Fifty-five percent of the sample is comprised of phenocrysts. Subhedral plagioclase phenocrysts comprise 40% of the sample and are up to 2.25 mm in length. Sericite along with alteration to calcite and chlorite is present on the plagioclase phenocrysts. Less than 1% of the plagioclase grains are completely replaced by calcite. Subhedral pyroxene phenocrysts comprise 10% of the sample and are up to 2 mm in length. Opaques are included in the both the plagioclase and pyroxene phenocrysts. Five percent of the sample is opaque anhedral phenocrysts that are up to 0.25 mm in size. The groundmass comprises 60 % of the sample and includes microphenocrysts in approximately the same proportion as the phenocrysts and also includes chlorite and calcite.</p>

Table 1. (continued)

Sample	Description
040709-10	Sample 040709-10 is a basaltic trachyandesite from Quebrada Buenaventura. Sixty-five percent of the sample is comprised of phenocrysts. Subhedral plagioclase phenocrysts are up to 2.8 mm and compose 50 % of the sample. Sericite is present on the plagioclase phenocrysts. Plagioclase phenocrysts are partially replaced by calcite and chlorite. Fifteen percent of the sample is comprised of anhedral pyroxene phenocrysts that are up to 2.9 mm in size. Reaction rims of opaques occur along the pyroxene phenocrysts. Plagioclase are included in pyroxene phenocrysts. Anhedral opaque phenocrysts are up to 0.5 mm in size. Some grains are replaced by calcite. The groundmass is composed of plagioclase, pyroxene, opaques, and less than 1% calcite and chlorite.
040709-13	Sample 040709-13 is an andesite from Quebrada Buenaventura. The sample contains 54% subhedral plagioclase phenocrysts that are up to 2 mm in size. Chlorite and sericite is present on plagioclase grains. Calcite replacement of grains occurs in 1% of the sample. Less than 1% of sample may be subhedral pyroxene phenocrysts up to 1.5 mm in size. The sample contains 45% groundmass, which is comprised of the same minerals and alteration products near the same proportion as in the phenocrysts, and includes a small amount of opaques.
040709-14	Sample 040709-14 is an andesite from Quebrada Buenaventura. Approximately 15% of the sample is comprised of phenocrysts. The phenocrysts display several intramineral fissures. Ten percent of the sample is subhedral feldspar phenocrysts are up to 2 mm in size. The plagioclase display sericite. Five percent of the phenocrysts are composed of what appears to have been euheral pyroxene phenocrysts, up to 0.75 mm in size, that are altered to a reddish brown material and reaction rims of opaques. Less than 1% of the phenocrysts are subhedral pyroxene up to 2 mm in size. Less than 1% of the phenocrysts are anhedral quartz up to 1 mm in size. The groundmass is comprised of cryptocrystalline material and opaques. The groundmass comprises 85% of the sample. In areas the groundmass appears to be the remnants of grains.

Table 1. (continued)

Sample	Description
040710-16	Sample 040710-16 is a dacite from Playa Soley. The phenocrysts comprise 40% of the section and are subhedral plagioclase phenocrysts that are up to 1.25 mm in length. The plagioclase phenocrysts are partially altered to chlorite. There appears to be reaction rims near the boundaries of some plagioclase phenocrysts. Less than 1% of the phenocrysts have been completely altered to calcite. The groundmass comprises 65% of the sample and consists of 40% cryptocrystalline material, 15% secondary opaques, 5% chlorite, and 5% areas of reddish brown alteration. Secondary opaques are up to 0.35 mm in size. Fissures cut across the section and may be filled with quartz, which may account for the difference between mineralogy and chemistry.
040710-19	Sample 040709-19 is defined by chemistry as a trachyandesite from Playa Soley. Approximately 50% of the sample consists of phenocrysts. Thirty-five percent of the section is altered subhedral plagioclase phenocrysts that are up to 1.75 mm in length. Approximately 1% of the phenocrysts have been completely replaced by calcite. Partial replacement of calcite is present on several grains. The majority of plagioclase phenocrysts have reddish brown alteration and inclusions of several alteration products. What may have been pyroxene phenocrysts, inferred from the grain boundaries, have been completely replaced alteration products and display reaction rims of opaques and reddish brown material. Other areas of the section consist of clusters of secondary opaques. The groundmass is approximately 40% of the section. This consists of secondary opaques, chlorite, and various alteration products. Fissures of calcite cross the section.

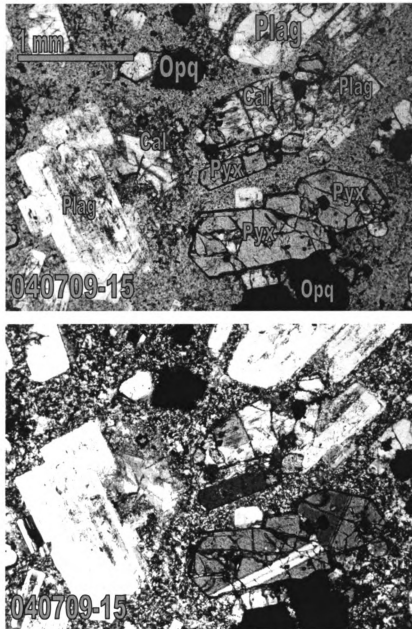


Figure 5. Photomicrograph of a lava sample, 040709-15, from Quebrada Buenaventura, in plane polarized light (top) and crossed polarized light (bottom). Plagioclase, pyroxene, and opaques form the phenocryst assemblage in lava samples from Punta Samara, Isla Paloma, and Quebrada Buenaventura, and 2 lava samples from Playa Soley (040710-16 and 040709-19). Plag is plagioclase, Pyx is pyroxene, Opq is opaque, and Cal is calcite.

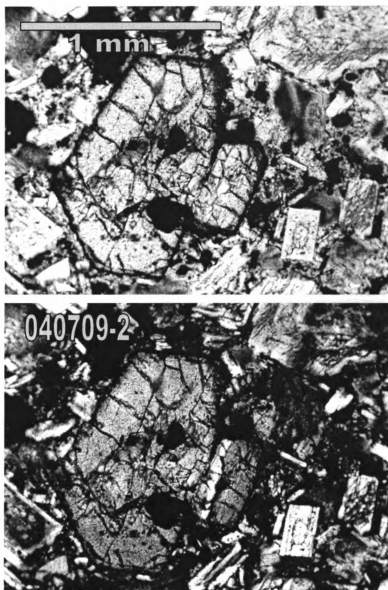


Figure 6. Photomicrograph of lava sample, 040709-2, from Quebrada Buenaventura, in plane polarized light (top), and cross polarized light (bottom). Reaction rims are present on some pyroxene grains.

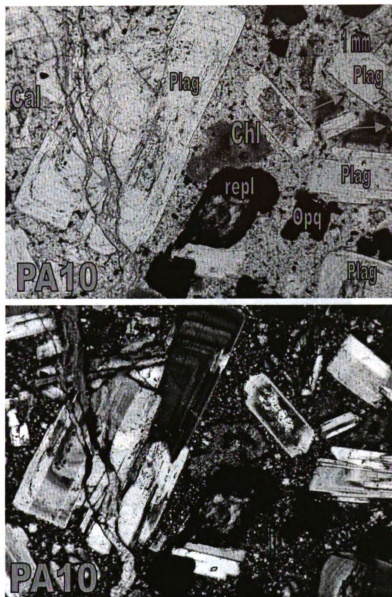


Figure 7. Photomicrograph of a lava sample, PA10, from Punta Samara, in plane polarized light (top) and crossed polarized light (bottom). Complete or partial replacement of grains by secondary products was present in some samples. Plag is plagioclase, Opq is opaque, Cal is calcite, Chl is chlorite, and repl is completely replaced grain.

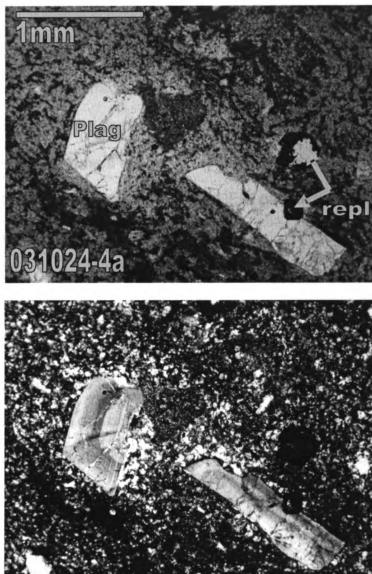


Figure 8. Photomicrograph of a fiamme sample, 031024-4a, from Playa Soley, in plane polarized light (top) and crossed polarized light (bottom). Anhedral feldspar and quartz form the phenocryst assemblage in fiamme samples from Playa Soley, and opaques appear to be secondary. Plag is plagioclase, Repl is completely replaced grain.

groundmass is comprised of microcrystalline material. The fiamme samples from Playa Soley generally contain a small percentage of anhedral phenocrysts of feldspar and quartz (Figure 9). The groundmass consists of microcrystalline material, which is most likely altered glass.

Alteration

When using geochemical data, particularly samples that have undergone mechanical weathering, the degree of chemical alteration must be considered. Low totals from major element analyses, the Weathering Index of Parker (WIP), and an evaluation of the rare earth element (REE) pattern were used to identify altered samples.

Low totals from major element analyses may have occurred due to improper sample preparation or due to alteration of the samples. The presence of clay minerals in altered samples results in lower sample totals as volatiles from these minerals escape during the fusing process. Samples that had totals below 96% were discarded from the rest of the geochemical analysis.

The Weathering Index of Parker (WIP) is based on the fraction of potassium, sodium, calcium, and magnesium present in the sample (Parker, 1970).

$$\text{WIP} = [(2 \times \text{Na}_2\text{O}/0.35) + (\text{MgO}/0.9) + (2\text{K}_2\text{O}/0.25) + (\text{CaO}/0.7)] \times 100$$

These elements are generally the most mobile of the major elements. The mobility of the individual alkali and alkaline earth elements is accounted for using the bond strength of the element to oxygen (Parker, 1970). Following Patino et

al. (2004), samples that had a WIP < 60 were discarded from the study. This value was chosen because samples with a WIP above 60 are comparable to the majority of the WIP values for the modern arc samples that are assumed to represent unweathered samples (Figure 9). Fifteen samples were excluded from the geochemical portion of the study using the WIP, including 7 ignimbrites and 8 lavas. The majority of the samples discarded using WIP were from Playa Soley. These samples have 78 to 84 wt% SiO₂, which also suggested alteration had occurred.

Even when alteration is not revealed by major element geochemistry, trace-element geochemistry might. Patino et al. (2003) studied weathering of corestone-shell complexes of basalt and andesites from Hawaii and Guatemala. Although the major element chemistry and petrographic analysis did not show signs of alteration, trace element patterns from the core and shell complexes indicated alteration when compared to other lavas from the same locations. Unusual REE patterns were observed in the remaining four ignimbrite samples from the primitive arc (Figure 10). For example, samples 031024-4a and 031024-4h, showed a slight negative Ce anomaly and an elevated REE pattern when compared to the rest of the sample set, and when compared to REE patterns from samples from the modern arc in Costa Rica. Patino et al. (2003) observed similar patterns in corestones, when compared to fresh lavas from their study area, and determined that this was due to alteration. The four ignimbrite samples with unusual REE patterns were excluded in the analysis.

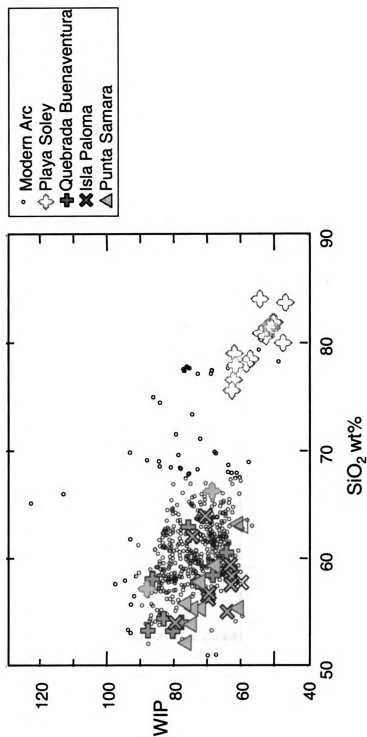


Figure 9. The majority of the modern arc samples (small open circles) from Costa Rica have WIP values greater than 60. Samples with WIP values less than 60 (open symbols) were not included in the geochemical interpretation.

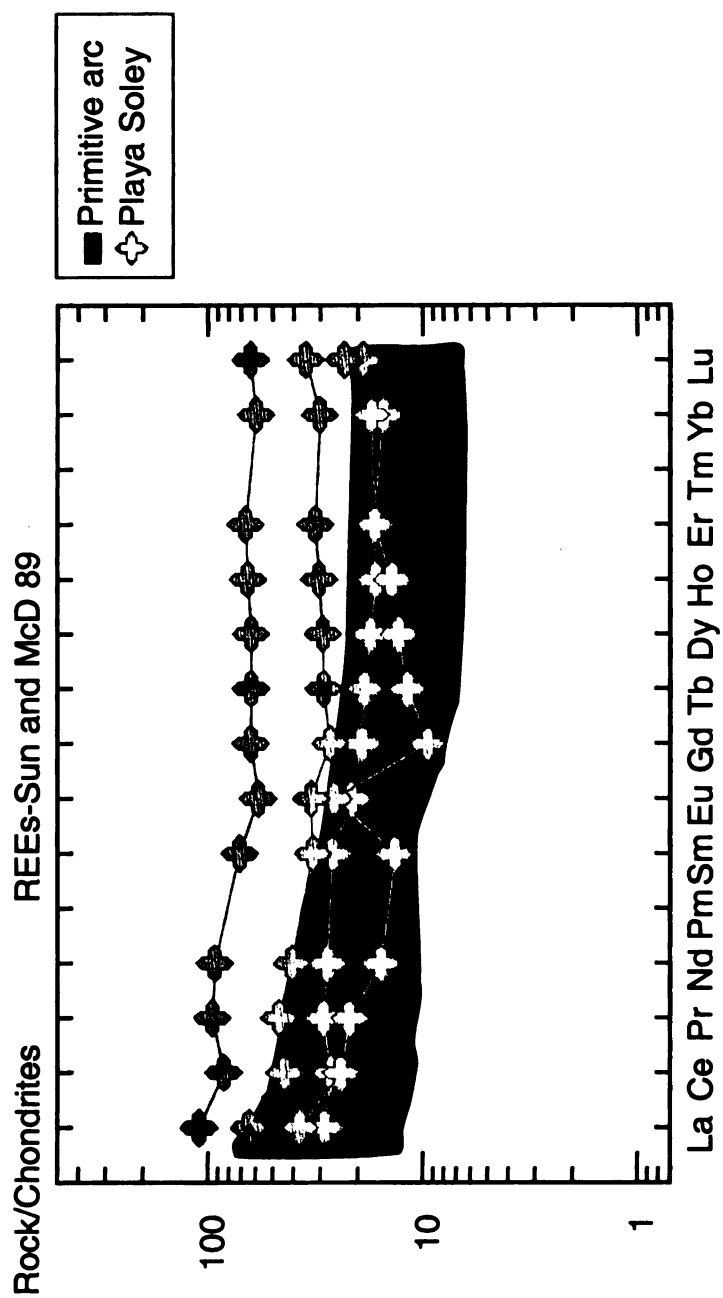


Figure 10. Pumice samples 031024-4a, 4b, 4e, and 4h had unusual REE patterns. These samples were not included in the geochemical portion of the study. The shaded area illustrates the REE patterns for the rest of the primitive arc samples.

Geochemistry

Whole rock major and trace element data for the lava samples from the primitive arc are listed in Table 2. All major element values discussed and in plots have been normalized to 100%. The total iron is presented as Fe_2O_3 . The samples from the primitive arc in Costa Rica range from basaltic to dacitic in composition (50.67 to 66.30 wt% SiO_2); some samples have higher alkali contents and are basaltic trachyandesite to trachyandesite in composition (Figure 11). The majority of the alkaline lava samples are from Quebrada Buenaventura.

The major element variations for samples from various locations are presented in Figure 12. MgO is relatively low, and ranges between 0.45 to 3.65 wt% for the samples from the primitive arc. The lava samples from the primitive arc have Al_2O_3 and Na_2O values between 15.45 and 21.17 wt% and 2.23 and 6.29 wt%, respectively. The samples from Punta Samara have the most similar Al_2O_3 (18.19 to 19.75 wt%) and Na_2O (2.70 to 4.26 wt%) compositions from the primitive arc. The values for K_2O vary between 0.50 to 2.54 wt% for the primitive arc volcaniclasts, and are more similar in Punta Samara (0.53 to 1.60 wt%), second only to Playa Soley (1.68 to 2.16 wt%), for which there are only two samples.

Trace-element concentrations for the samples are shown in Table 2. Figure 13 displays trace elements versus SiO_2 . Lavas from Punta Samara have a smaller range of values than the other sample locations for Nb, Ta, and Zr. The samples from the primitive arc are enriched in large ion lithophile elements (LILE) and depleted in high field strength elements (HFSE), which is

Table 2. Major (wt%) and trace element (ppm) concentrations for primitive arc volcanoclasts. Samples not collected in the 2004 field season originated from (#) Kennet Flores (and location is in the Costa Rican coordinate system), (+) Patino and others (2004), and (=) T.A. Vogel.

Sample	PA 040709-1	PA 040709-2	PA 040709-3	PA 040709-4
Latitude (N)	10.65	10.65	10.65	10.65
Longitude (W)	85.42	85.42	85.42	85.42
Location name	Quebrada Buenaventura	Quebrada Buenaventura	Quebrada Buenaventura	Quebrada Buenaventura
Sample type	lava	lava	lava	lava
SiO ₂	53.30	57.41	52.66	32.43
TiO ₂	0.93	0.84	0.97	0.68
Al ₂ O ₃	19.75	16.54	18.21	13.62
Fe ₂ O ₃	7.28	8.15	8.28	7.51
MnO	0.15	0.11	0.15	0.34
MgO	2.39	2.11	2.94	2.97
CaO	7.36	8.12	8.50	22.67
Na ₂ O	4.87	3.28	4.38	2.05
K ₂ O	1.60	1.44	0.99	0.13
P ₂ O ₅	0.26	0.20	0.24	0.16
Totals	97.89	98.20	97.32	82.56
Cu (XRF)	35.00	42.00	41.00	64.00
Zn (XRF)	53.00	36.00	71.00	65.00
Rb (XRF)	23.00	27.00	13.00	0.00
Sr (XRF)	461.00	342.00	357.00	300.00
Zr (XRF)	88.00	75.00	86.00	33.00
V	194.99	199.53	262.55	197.67
Cr	9.20	8.20	7.18	20.37
Y	23.88	22.03	31.54	17.58
Nb	3.27	1.88	2.08	1.32
Ba	573.55	454.08	535.30	129.99
La	9.18	5.99	7.32	5.99
Ce	19.20	12.97	16.66	9.82
Pr	3.07	2.09	2.77	1.60
Nd	14.52	10.25	13.68	8.00
Sm	4.05	3.15	4.04	2.44
Eu	1.25	1.08	1.32	0.80
Gd	4.16	3.46	4.65	2.69
Tb	0.65	0.57	0.76	0.42
Dy	3.81	3.54	4.86	2.72
Ho	0.85	0.81	1.11	0.60
Er	2.38	2.33	3.16	1.81
Yb	2.16	2.19	2.97	1.63
Lu	0.33	0.36	0.46	0.27
Hf	2.70	2.34	2.70	1.28
Ta	0.29	0.21	0.23	0.18
Pb	2.69	1.38	1.22	1.00
Th	1.21	0.52	0.59	0.30
U	0.59	0.16	0.20	0.18

Table 2. continued

Sample	PA 040709-5	PA 040709-6	PA 040709-9	PA 040709-10
Latitude (N)	10.65	10.65	10.65	10.65
Longitude (W)	85.42	85.42	85.42	85.42
Location name	Quebrada Buenaventura	Quebrada Buenaventura	Quebrada Buenaventura	Quebrada Buenaventura
Sample type	lava	lava	lava	lava
SiO₂	59.62	56.76	51.47	52.04
TiO₂	0.62	0.75	0.82	0.89
Al₂O₃	17.33	18.52	18.69	20.67
Fe₂O₃	7.78	5.11	7.32	6.46
MnO	0.10	0.08	0.12	0.17
MgO	1.71	2.27	2.89	1.74
CaO	6.30	6.96	8.38	9.82
Na₂O	3.81	4.69	4.91	4.49
K₂O	1.03	2.34	1.64	1.16
P₂O₅	0.14	0.22	0.25	0.22
Totals	98.44	97.70	96.49	97.66
Cu (XRF)	97.00	103.00	56.00	87.00
Zn (XRF)	33.00	34.00	67.00	49.00
Rb (XRF)	20.00	26.00	15.00	17.00
Sr (XRF)	402.00	362.00	399.00	401.00
Zr (XRF)	53.00	131.00	86.00	62.00
V	571.46	220.93	180.20	258.99
Cr	8.84	59.75	8.18	5.13
Y	9.74	19.06	18.58	23.07
Nb	1.38	4.05	2.84	1.54
Ba	489.33	762.20	623.44	581.21
La	4.13	11.57	8.50	5.50
Ce	8.38	25.42	18.02	12.55
Pr	1.20	3.58	2.82	2.09
Nd	5.66	15.39	12.96	10.33
Sm	1.97	3.83	3.30	3.38
Eu	0.76	1.02	1.08	1.13
Gd	1.89	3.59	3.38	3.63
Tb	0.30	0.52	0.51	0.60
Dy	1.88	3.19	3.06	3.80
Ho	0.41	0.63	0.65	0.83
Er	1.29	1.76	1.86	2.35
Yb	1.23	1.58	1.72	2.17
Lu	0.21	0.26	0.27	0.34
Hf	1.80	2.98	2.37	2.01
Ta	0.19	0.36	0.22	0.21
Pb	1.33	2.31	1.93	1.04
Th	0.51	1.94	1.20	0.46
U	0.24	0.88	0.38	0.20

Table 2. continued

Sample	PA 040709-12	PA 040709-13	PA 040709-14	17-5-1201
				#
Latitude (N)	10.65	10.65	10.65	242.75
Longitude (W)	85.42	85.42	85.42	410.35
Location name	Quebrada	Quebrada	Quebrada	Quebrada
	Buenaventura	Buenaventura	Buenaventura	Buenaventura
Sample type	lava	lava	lava	lava
SiO ₂	49.56	56.30	61.88	48.96
TiO ₂	0.78	0.75	0.69	0.78
Al ₂ O ₃	17.74	18.92	16.34	17.28
Fe ₂ O ₃	5.60	5.51	5.75	5.73
MnO	0.21	0.17	0.08	0.22
MgO	1.66	1.80	2.60	1.76
CaO	12.33	8.56	4.42	12.51
Na ₂ O	5.40	4.37	5.00	5.28
K ₂ O	0.90	0.75	1.38	0.90
P ₂ O ₅	0.22	0.20	0.18	0.22
Totals	94.40	97.33	98.32	93.64
Cu (XRF)	28.00	46.00	89.00	26.00
Zn (XRF)	67.00	64.00	54.00	67.00
Rb (XRF)	11.00	10.00	8.00	11.00
Sr (XRF)	366.00	381.00	371.00	357.00
Zr (XRF)	84.00	70.00	138.00	82.00
V	189.54	200.54	164.65	182.53
Cr	9.59	7.46	52.97	11.01
Y	19.74	20.01	19.18	20.59
Nb	1.95	1.13	4.48	2.11
Ba	479.84	575.23	911.73	454.13
La	7.04	4.97	11.87	7.24
Ce	16.11	12.61	24.59	15.96
Pr	2.49	1.97	3.63	2.53
Nd	11.76	9.41	15.71	12.05
Sm	3.16	2.86	4.25	3.54
Eu	1.04	0.99	1.17	1.14
Gd	3.18	2.88	3.95	3.51
Tb	0.49	0.47	0.60	0.54
Dy	3.20	3.38	3.72	3.49
Ho	0.66	0.68	0.76	0.73
Er	1.87	1.92	2.21	2.12
Yb	1.71	1.78	2.22	2.04
Lu	0.28	0.30	0.37	0.34
Hf	2.06	1.72	3.93	2.31
Ta	0.19	0.17	0.50	0.26
Pb	1.80	0.80	4.23	1.17
Th	0.74	0.41	2.96	0.78
U	0.35	0.21	1.02	0.46

Table 2. continued

Sample	PA 040709-15	PA 040709-16	PA 040709-17	PA 040709-18
Latitude (N)	10.11	10.11	10.11	10.11
Longitude (W)	85.20	85.20	85.20	85.20
Location name	Isla	Isla	Isla	Isla
	Paloma	Paloma	Paloma	Paloma
Sample type	lava	lava	lava	lava
SiO₂	59.77	62.29	55.82	55.39
TiO₂	0.66	0.71	0.80	0.63
Al₂O₃	15.24	15.04	18.07	17.51
Fe₂O₃	4.47	5.03	8.65	8.50
MnO	0.10	0.09	0.10	0.18
MgO	0.87	1.30	2.72	3.59
CaO	9.70	7.31	7.48	7.61
Na₂O	3.56	3.75	3.82	2.20
K₂O	1.77	1.68	1.02	2.50
P₂O₅	0.17	0.17	0.19	0.33
Totals	96.31	97.37	98.67	98.44
Cu (XRF)	22.00	47.00	59.00	166.00
Zn (XRF)	24.00	50.00	55.00	71.00
Rb (XRF)	24.00	24.00	19.00	35.00
Sr (XRF)	332.00	316.00	376.00	586.00
Zr (XRF)	132.00	140.00	62.00	55.00
V	169.76	175.24	168.37	173.75
Cr	14.65	11.97	5.63	5.33
Y	24.91	27.18	22.76	20.31
Nb	2.43	3.02	2.02	3.73
Ba	671.89	659.33	397.52	849.53
La	9.48	9.44	6.34	12.22
Ce	22.97	22.14	13.37	21.81
Pr	3.34	3.34	2.30	3.03
Nd	14.48	14.96	11.14	13.11
Sm	4.06	4.29	3.04	3.14
Eu	1.12	1.13	1.05	1.00
Gd	3.88	4.13	3.45	3.36
Tb	0.62	0.65	0.53	0.49
Dy	4.33	4.45	3.69	3.26
Ho	0.82	0.87	0.76	0.67
Er	2.29	2.47	2.08	1.92
Yb	2.16	2.33	1.96	1.87
Lu	0.37	0.38	0.33	0.31
Hf	2.96	3.38	1.83	1.66
Ta	0.34	0.33	0.18	0.28
Pb	2.63	2.89	1.02	2.99
Th	1.55	1.70	0.71	2.14
U	0.82	0.84	0.25	0.54

Table 2. continued

Sample	PA 040709-19	PA 040709-20	PA 040709-21	PA 040709-22
Latitude (N)	10.11	10.11	10.11	10.11
Longitude (W)	85.20	85.20	85.20	85.20
Location name	Isla	Isla	Isla	Isla
	Paloma	Paloma	Paloma	Paloma
Sample type	lava	lava	lava	lava
SiO₂	50.26	58.48	52.83	55.50
TiO₂	0.85	0.71	0.84	0.80
Al₂O₃	17.20	18.21	18.99	18.62
Fe₂O₃	6.74	7.29	7.03	6.16
MnO	0.25	0.15	0.16	0.25
MgO	1.96	2.97	2.14	1.78
CaO	11.72	7.48	10.17	10.03
Na₂O	4.74	3.46	4.52	3.72
K₂O	0.84	0.53	0.80	0.63
P₂O₅	0.22	0.19	0.23	0.20
Totals	94.78	99.47	97.71	97.69
Cu (XRF)	34.00	39.00	25.00	46.00
Zn (XRF)	65.00	64.00	79.00	70.00
Rb (XRF)	11.00	7.00	9.00	9.00
Sr (XRF)	336.00	398.00	426.00	393.00
Zr (XRF)	79.00	63.00	76.00	68.00
V	219.43	225.33	202.87	201.06
Cr	8.63	21.20	9.49	5.91
Y	25.52	19.62	20.09	21.83
Nb	1.80	1.44	2.16	1.38
Ba	456.62	486.87	459.56	489.90
La	6.09	4.70	6.67	5.32
Ce	13.91	10.92	15.09	12.03
Pr	2.28	1.83	2.59	1.95
Nd	11.17	9.04	12.05	9.56
Sm	3.17	2.87	3.78	2.70
Eu	1.06	0.97	1.09	0.96
Gd	3.46	3.06	3.35	3.02
Tb	0.56	0.50	0.53	0.48
Dy	3.98	3.17	3.37	3.42
Ho	0.81	0.69	0.70	0.73
Er	2.27	2.04	2.01	2.02
Yb	2.11	1.91	1.85	1.86
Lu	0.35	0.33	0.30	0.31
Hf	1.95	2.03	2.20	1.77
Ta	0.16	0.20	0.22	0.15
Pb	0.47	1.35	1.28	0.76
Th	0.40	0.46	0.65	0.39
U	0.16	0.19	0.30	0.17

Table 2. continued

Sample	PA 040709-24	PA 040709-25	PA 040709-26	14-11-1201
				#
Latitude (N)	10.11	10.11	10.11	241.7
Longitude (W)	85.20	85.20	85.20	339.8
Location name	Isla	Isla	Isla	Isla
	Paloma	Paloma	Paloma	Paloma
Sample type	lava	lava	lava	lava
SiO₂	57.26	54.84	56.80	58.35
TiO₂	0.86	0.75	0.59	0.73
Al₂O₃	16.42	19.00	19.14	18.48
Fe₂O₃	8.73	8.75	6.77	5.99
MnO	0.21	0.21	0.16	0.18
MgO	3.58	3.50	2.09	1.88
CaO	6.94	8.79	9.17	8.25
Na₂O	2.98	3.06	2.85	3.57
K₂O	0.96	0.50	0.57	0.55
P₂O₅				
	0.16	0.16	0.17	0.20
Totals	98.10	99.56	98.31	98.18
Cu (XRF)	73.00	36.00	46.00	22.00
Zn (XRF)	106.00	72.00	66.00	65.00
Rb (XRF)	12.00	6.00	8.00	9.00
Sr (XRF)	304.00	404.00	405.00	416.00
Zr (XRF)	96.00	45.00	33.00	74.00
V	226.30	277.38	185.19	177.18
Cr	5.78	8.04	4.64	7.30
Y	28.80	18.45	15.41	23.83
Nb	6.11	0.84	0.68	1.33
Ba	585.06	413.32	465.92	510.39
La	8.25	3.70	3.81	5.57
Ce	17.53	8.67	8.56	12.71
Pr	2.66	1.48	1.39	2.07
Nd	12.31	7.44	6.92	10.17
Sm	3.37	2.18	2.09	2.86
Eu	0.97	0.81	0.74	0.98
Gd	3.82	2.50	2.25	3.25
Tb	0.62	0.41	0.34	0.51
Dy	4.12	2.82	2.42	3.65
Ho	0.92	0.61	0.50	0.75
Er	2.62	1.70	1.44	2.13
Yb	2.44	1.60	1.30	1.94
Lu	0.38	0.27	0.23	0.34
Hf	2.55	1.24	1.03	1.96
Ta	0.41	0.10	0.10	0.15
Pb	2.64	0.39	0.56	0.72
Th	1.30	0.27	0.30	0.46
U	0.41	0.10	0.12	0.22

Table 2. continued

Sample	13-11-1201	PA 040710-12	PA 040710-14	PA 040710-15
	#			
Latitude (N)	241.7	11.04	11.04	11.04
Longitude (W)	339.8	85.67	85.67	85.67
Location name	Isla	Playa	Playa	Playa
	Paloma	Soley	Soley	Soley
Sample type	lava	lava	lava	lava
SiO₂	56.29	83.22	82.39	79.97
TiO₂	0.79	0.26	0.33	0.33
Al₂O₃	18.10	9.54	10.59	10.39
Fe₂O₃	7.00	0.35	0.48	0.80
MnO	0.15	0.01	0.01	0.01
MgO	2.26	0.00	0.04	0.14
CaO	9.34	1.00	1.47	1.35
Na₂O	3.11	3.12	3.21	3.20
K₂O	0.56	1.82	1.97	2.08
P₂O₅	0.17	0.05	0.08	0.06
Totals	97.77	99.37	100.57	98.33
Cu (XRF)	14.00	bd	11.00	bd
Zn (XRF)	50.00	bd	32.00	bd
Rb (XRF)	10.00	23.90	30.00	31.40
Sr (XRF)	327.00	90.30	120.00	116.00
Zr (XRF)	63.00	142.50	140.00	146.10
V	190.19	35.16	47.49	74.64
Cr	6.05	28.18	13.44	18.40
Y	22.37	24.55	26.90	26.71
Nb	1.26	4.45	2.32	4.05
Ba	386.50	560.36	595.64	668.53
La	4.54	8.27	9.10	6.68
Ce	10.59	19.17	20.21	13.92
Pr	1.75	2.83	3.00	1.94
Nd	8.77	10.06	13.30	5.99
Sm	2.63	2.91	3.68	1.99
Eu	0.98	0.97	0.98	1.02
Gd	3.10	2.93	3.78	2.15
Tb	0.49	0.61	0.62	0.54
Dy	3.59	3.75	5.98	3.36
Ho	0.72	0.91	0.94	0.93
Er	2.02	2.78	2.70	2.92
Yb	1.80	2.89	2.72	2.90
Lu	0.31	0.57	0.54	0.59
Hf	1.70	3.68	3.81	4.05
Ta	0.15	1.13	0.69	1.04
Pb	0.27	8.29	1.72	10.08
Th	0.34	2.19	2.00	2.22
U	0.13	3.21	0.98	3.49

Table 2. continued

Sample	PA 040710-16	PA 040710-17	PA 040710-19	PA 040710-20
Latitude (N)	11.04	11.04	11.04	11.04
Longitude (W)	85.67	85.67	85.67	85.67
Location name	Playa	Playa	Playa	Playa
	Soley	Soley	Soley	Soley
Sample type	lava	lava	lava	ignimbrite
SiO₂	65.37	80.11	55.35	80.82
TiO₂	0.72	0.32	0.63	0.27
Al₂O₃	16.48	10.62	17.63	11.08
Fe₂O₃	4.48	0.49	7.80	0.50
MnO	0.03	0.01	0.13	0.01
MgO	0.44	0.00	0.74	0.08
CaO	4.58	1.38	6.55	1.54
Na₂O	4.15	3.34	6.09	3.73
K₂O	2.13	1.97	1.63	1.82
P₂O₅	0.21	0.06	0.22	0.06
Totals	98.59	98.30	96.77	99.91
Cu (XRF)	bd	bd	bd	10.00
Zn (XRF)	bd	bd	bd	9.00
Rb (XRF)	44.50	22.10	21.90	22.00
Sr (XRF)	469.70	119.50	310.70	117.00
Zr (XRF)	149.70	140.20	58.90	108.00
V	189.78	36.93	118.01	21.60
Cr	39.33	10.77	8.93	8.19
Y	17.59	28.60	16.64	21.55
Nb	4.69	2.95	1.19	1.80
Ba	723.15	618.59	552.36	431.72
La	13.33	8.98	4.01	5.14
Ce	28.78	20.32	8.89	12.37
Pr	4.02	2.97	1.40	1.80
Nd	17.08	12.79	7.05	8.13
Sm	3.83	3.60	2.13	2.63
Eu	1.16	0.95	0.80	0.75
Gd	3.46	3.58	2.14	2.80
Tb	0.53	0.66	0.38	0.50
Dy	3.10	4.41	2.44	5.09
Ho	0.62	1.01	0.52	0.74
Er	1.78	3.12	1.54	2.26
Yb	1.82	3.07	1.40	2.17
Lu	0.29	0.59	0.23	0.48
Hf	3.94	4.10	1.69	2.98
Ta	0.47	0.80	0.12	0.51
Pb	5.44	8.05	1.22	0.32
Th	2.30	2.35	0.19	1.60
U	1.17	1.78	0.20	1.02

Table 2. continued

Sample	PA 040710-23	031024-4a	031024-4b	031024-4c
		=	=	=
Latitude (N)	11.04	11.04	11.04	11.04
Longitude (W)	85.67	85.67	85.67	85.67
Location name	Playa	Playa	Playa	Playa
	Soley	Soley	Soley	Soley
Sample type	ignimbrite	ignimbrite	ignimbrite	ignimbrite
SiO₂	81.01	75.64	74.53	77.73
TiO₂	0.24	0.55	0.61	0.35
Al₂O₃	10.93	12.62	13.40	12.18
Fe₂O₃	0.47	1.74	1.33	0.91
MnO	0.01	0.02	0.01	0.01
MgO	0.04	0.26	0.29	0.09
CaO	1.42	1.44	2.00	1.86
Na₂O	3.73	4.71	5.13	4.08
K₂O	1.66	1.72	1.16	1.73
P₂O₅	0.06	0.08	0.14	0.07
Totals	99.57	98.78	98.60	99.01
Cu (XRF)	19.00			
Zn (XRF)	13.00			
Rb (XRF)	20.00	30.00	14.30	15.90
Sr (XRF)	118.00	170.90	183.70	149.20
Zr (XRF)	100.00	170.70	99.50	111.60
V	23.36	48.12	67.45	37.49
Cr	7.78	9.77	14.81	14.77
Y	24.66	129.79	27.85	42.07
Nb	1.31	3.80	2.78	2.36
Ba	423.97	503.57	389.48	545.84
La	5.18	25.93	6.76	10.62
Ce	11.78	51.33	16.29	17.92
Pr	1.89	9.05	2.74	3.35
Nd	8.61	43.18	12.97	14.66
Sm	2.75	10.87	4.03	4.02
Eu	0.73	3.38	1.24	1.25
Gd	3.15	12.97	3.96	4.48
Tb	0.54	2.35	0.70	0.84
Dy	5.30	15.96	4.47	5.82
Ho	0.79	3.68	0.94	1.35
Er	2.40	11.04	2.82	4.16
Yb	2.12	10.13	2.60	4.02
Lu	0.49	1.61	0.48	0.73
Hf	2.89	5.01	3.13	3.62
Ta	0.50	0.60	0.48	0.56
Pb	0.17	7.49	5.14	4.49
Th	1.57	1.80	1.35	1.99
U	0.91	1.37	1.37	1.63

Table 2. continued

Sample	031024-4d	031024-4e	031024-4f	031024-4g
	=	=	=	=
Latitude (N)	11.04	11.04	11.04	11.04
Longitude (W)	85.67	85.67	85.67	85.67
Location name	Playa	Playa	Playa	Playa
	Soley	Soley	Soley	Soley
Sample type	ignimbrite	ignimbrite	ignimbrite	ignimbrite
SiO₂	79.73	78.12	80.70	77.11
TiO₂	0.35	0.40	0.32	0.36
Al₂O₃	11.13	11.84	10.32	12.63
Fe₂O₃	0.52	0.71	0.47	0.57
MnO	0.01	0.01	0.01	0.01
MgO	0.00	0.11	0.00	0.00
CaO	1.68	1.10	1.40	2.09
Na₂O	3.58	4.20	3.47	4.51
K₂O	1.81	2.36	1.77	1.39
P₂O₅	0.07	0.01	0.06	0.12
Totals	98.88	98.86	98.52	98.79
Cu (XRF)				
Zn (XRF)				
Rb (XRF)	26.70	35.40	24.50	11.00
Sr (XRF)	146.70	145.00	133.60	156.40
Zr (XRF)	135.50	186.90	133.10	107.80
V	64.68	53.15	29.55	35.24
Cr	15.61	13.34	9.06	17.54
Y	30.68	23.84	30.49	26.51
Nb	3.11	4.22	2.54	2.27
Ba	677.95	557.53	631.66	470.43
La	8.55	8.83	9.48	7.78
Ce	17.64	14.67	21.01	17.55
Pr	2.54	2.08	3.02	3.06
Nd	10.19	7.27	13.14	14.07
Sm	2.82	2.05	3.65	4.09
Eu	1.03	1.50	0.95	1.22
Gd	3.00	1.94	3.69	4.04
Tb	0.63	0.44	0.70	0.74
Dy	4.46	3.30	4.74	4.39
Ho	0.99	0.79	1.02	0.96
Er	3.29	2.78	3.30	2.90
Yb	3.21	2.95	3.45	2.77
Lu	0.59	0.59	0.60	0.51
Hf	4.22	5.33	4.33	3.33
Ta	0.92	0.81	0.75	0.53
Pb	7.58	5.79	7.57	4.65
Th	2.12	2.02	2.38	1.81
U	2.33	1.71	1.61	2.03

Table 2. continued

Sample	031024-4h	031024-4l	PD3-21-0202	PD1-21-0202
	=	=	#	#
Latitude (N)	11.04	11.04	336.3	336.3
Longitude (W)	85.67	85.67	348.0	348.0
Location name	Playa	Playa	Playa	Playa
	Soley	Soley	Rajada	Rajada
Sample type	ignimbrite	ignimbrite	lava	lava
SiO₂	76.56	80.16	84.28	79.99
TiO₂	0.40	0.29	0.22	0.58
Al₂O₃	11.84	10.43	9.20	11.51
Fe₂O₃	1.56	0.54	0.51	0.62
MnO	0.03	0.01	0.01	0.05
MgO	0.11	0.01	0.01	0.00
CaO	1.22	1.39	0.91	1.48
Na₂O	4.42	3.56	2.90	4.86
K₂O	2.06	1.77	2.16	0.73
P₂O₅	0.06	0.06	0.04	0.17
Totals	98.26	98.22	100.24	99.99
Cu (XRF)			0.00	7.00
Zn (XRF)			15.00	33.00
Rb (XRF)	36.30	19.20	36.00	10.00
Sr (XRF)	147.10	127.50	84.00	154.00
Zr (XRF)	182.00	129.40	134.00	119.00
V	27.27	18.90	29.20	31.99
Cr	8.98	19.53	7.54	9.06
Y	55.73	25.64	19.05	64.23
Nb	2.96	2.68	2.31	1.29
Ba	554.45	600.55	562.68	370.01
La	15.18	6.71	7.22	9.32
Ce	26.93	14.22	15.88	22.68
Pr	4.42	2.12	2.12	4.09
Nd	18.96	7.76	8.46	20.81
Sm	4.97	2.36	2.34	6.59
Eu	1.92	0.97	0.67	1.83
Gd	5.55	2.51	2.39	7.90
Tb	1.08	0.56	0.40	1.36
Dy	7.41	3.61	4.26	10.68
Ho	1.72	0.90	0.63	2.00
Er	5.22	2.74	1.97	5.38
Yb	5.11	2.84	2.04	4.80
Lu	0.89	0.53	0.44	0.85
Hf	5.45	4.02	3.20	4.25
Ta	0.64	0.65	0.79	0.46
Pb	2.19	10.31	1.22	0.78
Th	2.04	2.24	2.23	1.04
U	1.37	2.01	0.96	0.66

Table 2. continued

Sample	031024-4h	031024-4i	PD3-21-0202	PD1-21-0202
	=	=	#	#
Latitude (N)	11.04	11.04		
Longitude (W)	85.67	85.67		
Location name	Playa	Playa	Playa	Playa
	Soley	Soley	Rajada	Rajada
Sample type	ignimbrite	ignimbrite	lava	lava
SiO₂	76.56	80.16	84.28	79.99
TiO₂	0.40	0.29	0.22	0.58
Al₂O₃	11.84	10.43	9.20	11.51
Fe₂O₃	1.56	0.54	0.51	0.62
MnO	0.03	0.01	0.01	0.05
MgO	0.11	0.01	0.01	0.00
CaO	1.22	1.39	0.91	1.48
Na₂O	4.42	3.56	2.90	4.86
K₂O	2.06	1.77	2.16	0.73
P₂O₅	0.06	0.06	0.04	0.17
Totals	98.26	98.22	100.24	99.99
Cu (XRF)			0.00	7.00
Zn (XRF)			15.00	33.00
Rb (XRF)	36.30	19.20	36.00	10.00
Sr (XRF)	147.10	127.50	84.00	154.00
Zr (XRF)	182.00	129.40	134.00	119.00
V	27.27	18.90	29.20	31.99
Cr	8.98	19.53	7.54	9.06
Y	55.73	25.64	19.05	64.23
Nb	2.96	2.68	2.31	1.29
Ba	554.45	600.55	562.68	370.01
La	15.18	6.71	7.22	9.32
Ce	26.93	14.22	15.88	22.68
Pr	4.42	2.12	2.12	4.09
Nd	18.96	7.76	8.46	20.81
Sm	4.97	2.36	2.34	6.59
Eu	1.92	0.97	0.67	1.83
Gd	5.55	2.51	2.39	7.90
Tb	1.08	0.56	0.40	1.36
Dy	7.41	3.61	4.26	10.68
Ho	1.72	0.90	0.63	2.00
Er	5.22	2.74	1.97	5.38
Yb	5.11	2.84	2.04	4.80
Lu	0.89	0.53	0.44	0.85
Hf	5.45	4.02	3.20	4.25
Ta	0.64	0.65	0.79	0.46
Pb	2.19	10.31	1.22	0.78
Th	2.04	2.24	2.23	1.04
U	1.37	2.01	0.96	0.66

Table 2. continued

Sample	PA5	PA6	PA8	PA9
	+	+	+	+
Latitude (N)				
Longitude (W)				
Location name	Punta	Punta	Punta	Punta
	Samara	Samara	Samara	Samara
Sample type	lava	lava	lava	lava
SiO₂	62.19	54.16	48.39	50.24
TiO₂	0.69	0.89	1.03	0.83
Al₂O₃	17.90	18.53	17.44	18.88
Fe₂O₃	4.91	7.99	9.00	7.80
MnO	0.05	0.10	0.24	0.14
MgO	0.70	1.86	3.03	1.73
CaO	7.19	9.32	11.83	11.61
Na₂O	3.64	3.68	3.45	3.20
K₂O	0.90	1.13	0.84	1.54
P₂O₅	0.23	0.18	0.25	0.24
Totals	98.40	97.84	95.50	96.21
Cu (XRF)	95.00	42.80	78.50	64.80
Zn (XRF)	49.10	77.00	89.20	82.70
Rb (XRF)	12.80	22.90	19.30	31.00
Sr (XRF)	554.60	535.10	472.00	550.10
Zr (XRF)	92.00	60.70	79.40	64.10
V				
Cr	-0.50	256.90	13.50	13.20
Y	14.37	20.15	23.41	19.74
Nb	2.92	1.67	2.42	2.03
Ba	676.04	420.63	383.26	501.55
La	7.29	7.39	6.74	8.14
Ce	18.39	15.58	16.11	17.25
Pr	2.50	2.37	2.61	2.62
Nd	10.34	10.69	12.26	11.71
Sm	2.58	2.88	3.23	2.97
Eu	1.00	1.01	1.19	1.10
Gd	2.69	3.22	3.60	3.12
Tb	0.46	0.55	0.62	0.54
Dy	2.12	3.02	3.60	3.10
Ho	0.45	0.62	0.74	0.61
Er	1.45	2.09	2.37	2.04
Yb	1.40	2.16	2.24	1.92
Lu	0.22	0.34	0.33	0.31
Hf	1.96	1.61	2.08	1.65
Ta	0.16	0.13	0.14	0.12
Pb	3.62	2.07	1.88	2.12
Th	0.74	0.52	0.52	0.82
U	0.37	0.18	0.21	0.26

Table 2. continued

Sample	PA10	PA11	PA12	PA13
	+	+	+	+
Latitude (N)				
Longitude (W)				
Location name	Punta	Punta	Punta	Punta
	Samara	Samara	Samara	Samara
Sample type	lava	lava	lava	lava
SiO₂	61.64	56.46	59.09	53.78
TiO₂	0.47	0.83	0.86	0.73
Al₂O₃	16.28	19.28	19.12	18.10
Fe₂O₃	6.57	5.21	6.20	6.49
MnO	0.12	0.10	0.07	0.23
MgO	1.39	0.91	0.97	1.20
CaO	6.86	9.45	8.16	11.60
Na₂O	3.33	3.91	3.78	3.67
K₂O	0.91	1.20	1.15	1.00
P₂O₅	0.16	0.25	0.18	0.33
Totals	97.73	97.60	99.58	97.13
Cu (XRF)	42.30	75.30	99.40	83.80
Zn (XRF)	67.30	86.10	87.50	73.10
Rb (XRF)	13.60	23.20	19.80	18.00
Sr (XRF)	503.20	511.90	503.60	591.30
Zr (XRF)	66.50	94.10	94.00	87.30
V				
Cr	-0.10	4.40	10.40	2.80
Y	12.97	23.46	22.65	22.63
Nb	1.72	2.72	2.78	2.80
Ba	594.68	566.04	535.88	613.50
La	5.85	8.54	7.15	10.62
Ce	13.27	20.41	17.88	21.49
Pr	1.99	3.13	2.93	3.06
Nd	8.79	13.83	13.78	12.79
Sm	2.22	3.55	3.73	3.08
Eu	0.86	1.29	1.26	1.13
Gd	2.30	3.73	3.80	3.24
Tb	0.42	0.63	0.67	0.57
Dy	1.91	3.45	3.71	3.05
Ho	0.37	0.68	0.73	0.62
Er	1.15	2.38	2.36	2.05
Yb	1.27	2.20	2.20	2.06
Lu	0.21	0.33	0.33	0.32
Hf	1.62	2.24	2.52	2.14
Ta	0.09	0.16	0.16	0.16
Pb	2.95	3.31	2.53	2.54
Th	0.59	0.71	0.76	0.92
U	0.18	0.41	0.36	0.31

Table 2. continued

Sample	PA14	PA15	PA18	PA19
	+	+	+	+
Latitude (N)				
Longitude (W)				
Location name	Punta Samara	Punta Samara	Punta Samara	Punta Samara
Sample type	lava	lava	lava	lava
SiO₂	51.78	54.99	54.47	27.95
TiO₂	0.73	0.71	0.87	0.39
Al₂O₃	18.17	19.21	18.82	10.35
Fe₂O₃	6.29	8.58	6.89	3.91
MnO	0.27	0.17	0.10	0.28
MgO	1.63	2.87	2.01	1.30
CaO	12.71	9.36	8.58	37.81
Na₂O	3.40	2.68	4.15	1.98
K₂O	0.83	0.53	1.34	0.48
P₂O₅	0.22	0.14	0.26	0.10
Totals	96.03	99.24	97.49	84.55
Cu (XRF)	69.70	169.10	125.00	49.30
Zn (XRF)	70.60	86.10	79.00	41.30
Rb (XRF)	13.20	10.00	24.20	7.50
Sr (XRF)	488.80	425.70	757.20	522.60
Zr (XRF)	73.70	43.70	95.80	34.40
V				
Cr	5.20	9.00	19.00	21.70
Y	20.11	16.84	14.23	5.52
Nb	2.17	1.06	2.98	1.01
Ba	472.90	434.25	600.55	297.80
La	7.78	4.24	8.03	3.00
Ce	17.35	9.72	17.58	6.58
Pr	2.67	1.59	2.61	0.92
Nd	11.44	7.61	11.13	3.71
Sm	2.94	2.20	2.73	0.96
Eu	1.12	0.89	1.23	0.41
Gd	3.13	2.48	2.77	1.27
Tb	0.53	0.49	0.48	0.22
Dy	3.02	2.51	2.30	0.72
Ho	0.60	0.53	0.45	0.13
Er	1.83	1.65	1.45	0.38
Yb	1.91	1.76	1.43	0.76
Lu	0.28	0.29	0.22	0.10
Hf	1.82	1.13	2.32	0.43
Ta	0.13	0.06	0.18	0.08
Pb	2.32	1.51	3.57	1.81
Th	0.78	0.44	1.38	0.18
U	0.36	0.17	0.47	0.86

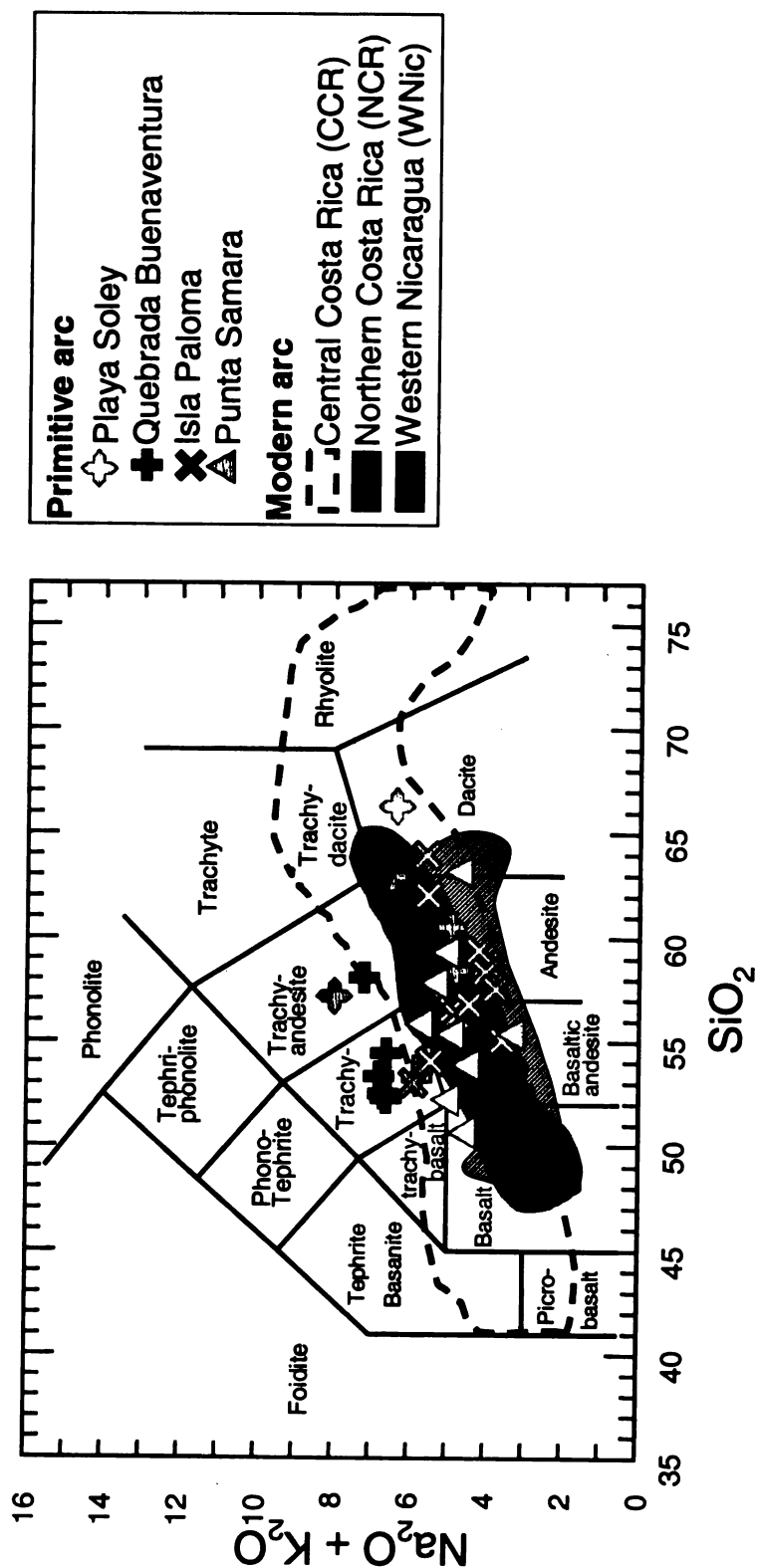


Figure 11. Total alkalis versus SiO_2 classification diagram of Le Bas et al. (1986) of the primitive arc volcanoclasts.

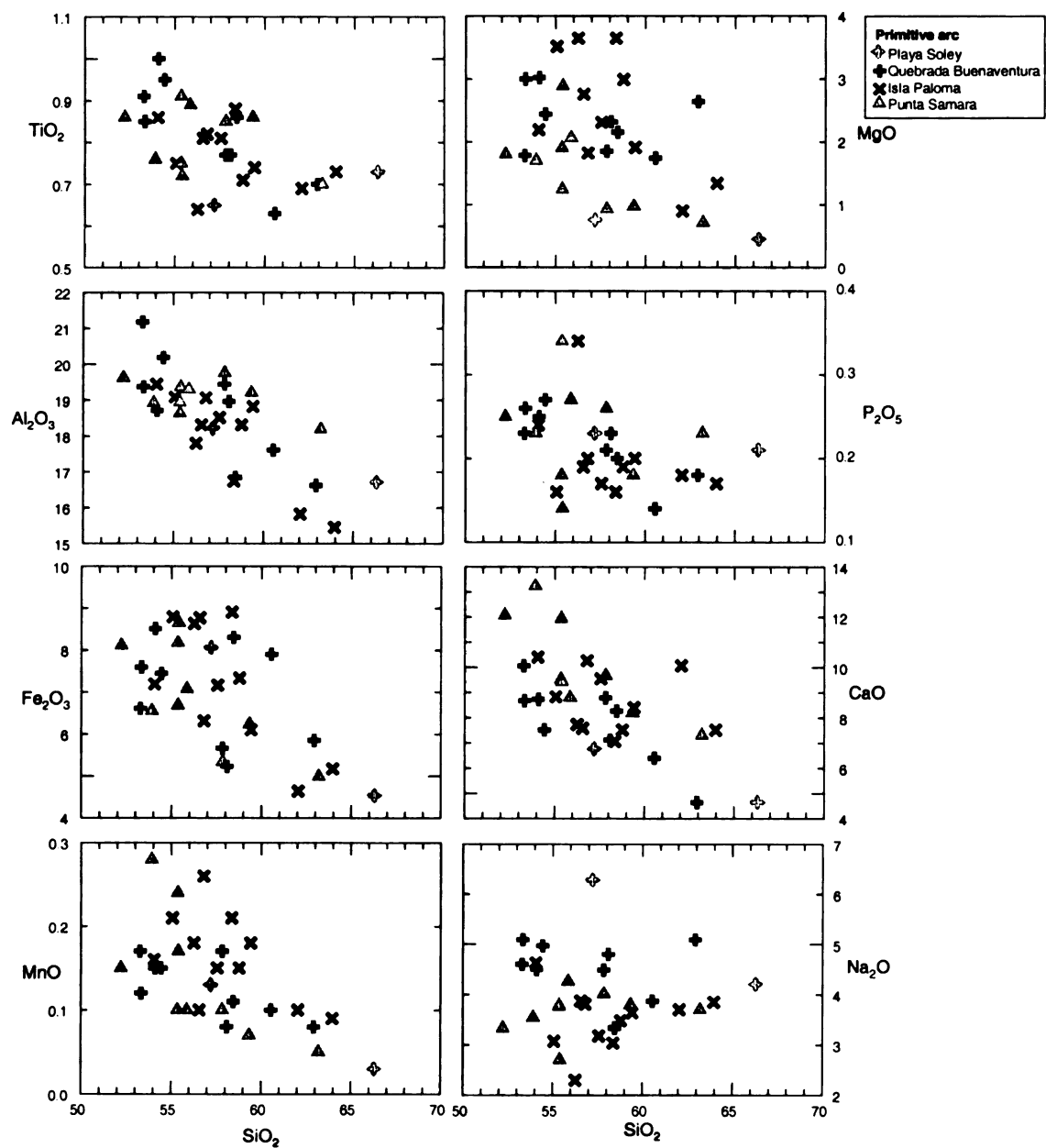


Figure 12. Major element variation versus SiO₂ (wt%) amongst the primitive arc lava samples.

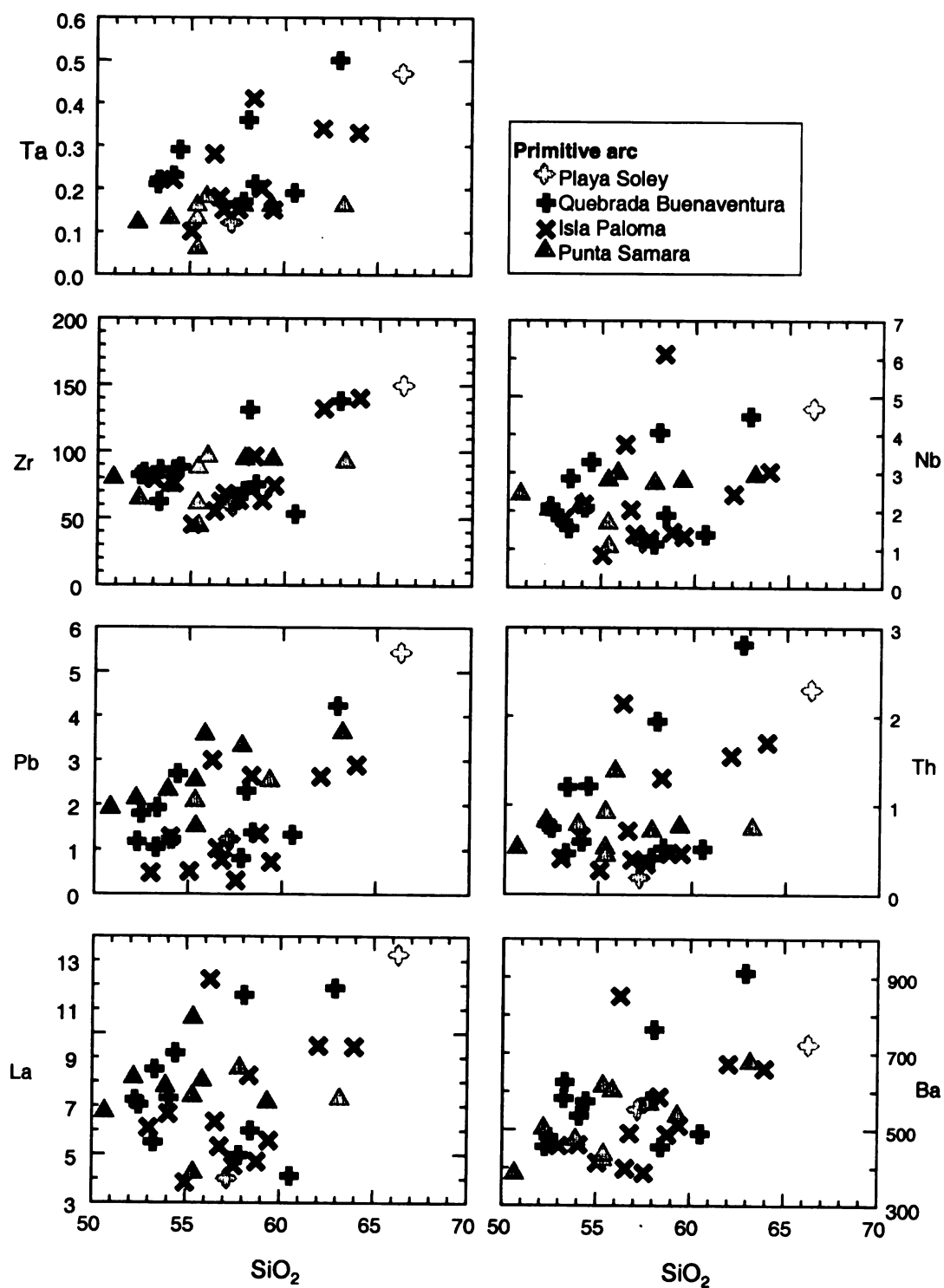


Figure 13. Trace element concentrations (ppm) versus SiO_2 (wt%) for the primitive arc lava samples.

characteristic of subduction zone related magmas (Figure 14). The rare earth element (REE) trends (Figure 15) are relatively similar to each other and are slightly more enriched in light rare earth elements (LREE) than heavy rare earth elements (HREE).

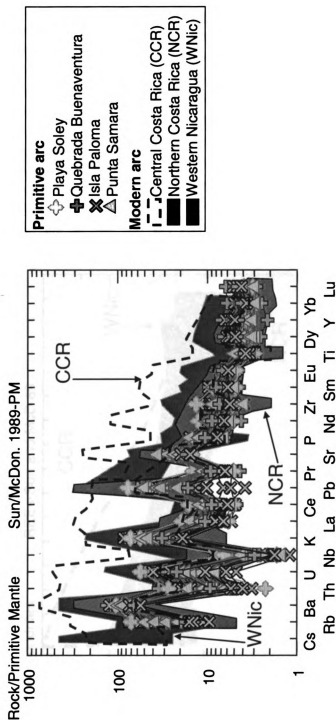


Figure 14. The spider diagram, normalized to the primitive mantle after Sun and McDonough (1989), illustrates that the primitive arc lavas samples are enriched in LILE relative to HFSE, characteristic of volcanics originated from subduction zone magmatism.

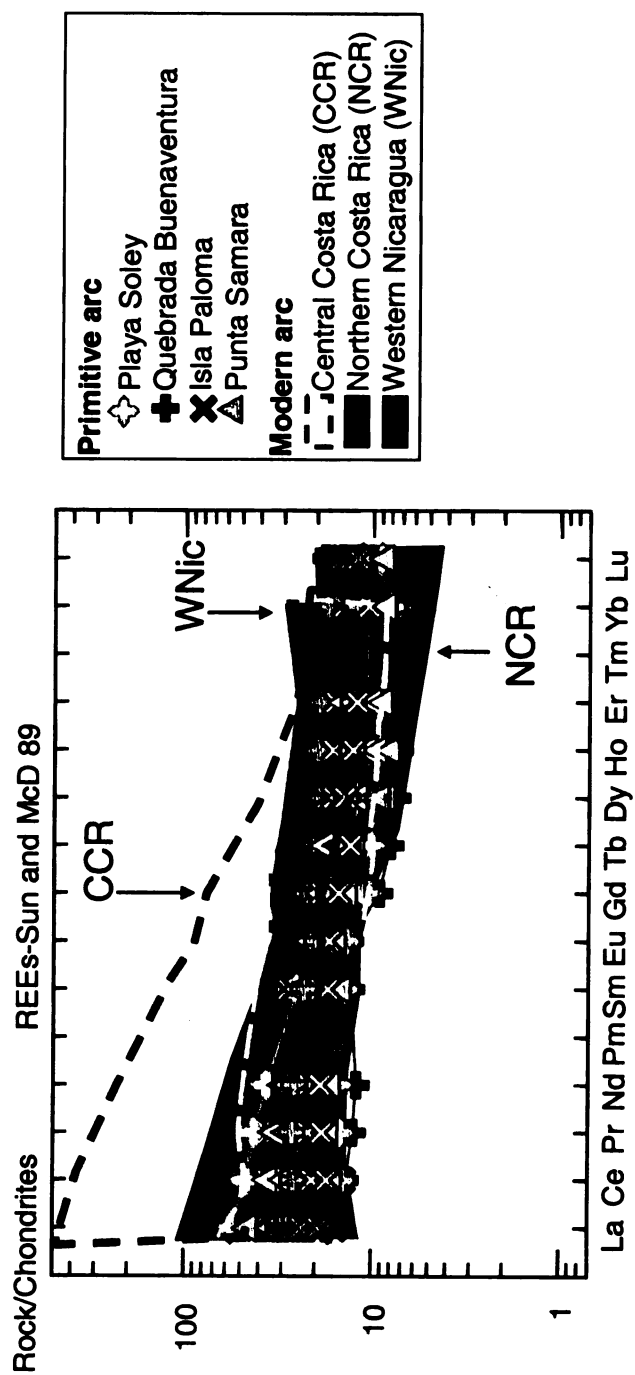


Figure 15. REE trend for the lava samples from the primitive arc are relatively similar to each other. Normalized to chondrite after Sun and McDonaugh (1989).

DISCUSSION

The major element variations (Figure 12) for these samples cannot be evaluated for fractional crystallization trends because these samples are volcaniclasts in a sedimentary deposit and the origin and relation of the lava clasts is unknown. However several inferences about the subduction parameters can still be made. Useful ratios and their ranges for each sample location are given in Table 3.

Mantle Source

Trace element data can be used to determine mantle source (Woodhead et al., 1998; Abratis and Worner, 2000). Dewatering of the subducting slab does not seem to affect the Zr/Nb ratio and it has been used to discriminate between mantle sources in arc related magmas (Woodhead et al., 1998; Abratis and Worner, 2000). Woodhead et al. (1998) proposed that the mantle source in the Marianas influenced the Zr/Nb ratio. In southern Costa Rica, Abratis and Worner (2000) determined that the volcanics originated from a more enriched mantle source based on the Zr/Nb ratios. Zirconium is less incompatible than Nb in mantle minerals (Sun and McDonough, 1989), and in a partial melt of the mantle, niobium will strongly partition to the melt. This leaves the mantle enriched in zirconium relative to niobium. Therefore, a high Zr/Nb ratio is indicative of a depleted mantle source, while a low Zr/Nb ratio variation signifies an enriched mantle source. Thus, the Zr/Nb ratio of the volcanic products also can give an indication as to how heterogeneous the mantle source is.

Table 3. Useful ranges of trace element ratios.

Ratio	Punta Samara	Isla Paloma	Quebrada Buenaventura	Playa Soley
Zr/Nb	31.2 - 41.2	14.7 - 55.6	26.9 - 61.9	31.9 - 49.5
Ba/La	56.9 - 102.4	62.7 - 111.7	62.5 - 118.5	54.3 - 137.8
La/Yb	2.4 - 5.6	2.3 - 6.5	2.5 - 7.3	2.9 - 7.3
Ba/Th	435.2 - 986.9	387.8 - 1530.8	5.8 - 15.8	314.4 - 2907.2
U/Th	0.32 - 0.58	0.25 - 0.53	0.31 - 0.59	0.51 - 1.05
Ce/Pb	4.9 - 8.6	6.6 - 39.2	308.0 - 1403.0	7.3 - 5.3

The primitive arc volcaniclasts have Zr/Nb ratios ranging from 15 to 62 (Figure 16). Patino et al. (2004) presented that the Zr/Nb ratios for lava clasts from Punta Samara have a close range of values, and conclude that these volcanic products originate from a homogenous mantle source. The homogeneity in mantle source for Punta Samara is a contrast to the other sample locations from the primitive arc included in this study. The Zr/Nb ratios are more variable within each sample location, and indicate a more heterogeneous mantle source than that found for volcaniclasts from Punta Samara (Figure 16). The lavas from the primitive arc have a predominately depleted mantle source influence. However, two lava samples from Isla Paloma, 040709-18 and 040709-24, have the lowest Zr/Nb ratio, indicating that these two samples have a more enriched mantle component contributing to the source of some of the primitive arc volcanics.

In the modern arc, the volcanics from central and northern Costa Rica have Zr/Nb ratios that range between approximately 10 to 19 and 5 to 70, respectively (Figure 16)(Carr et al., 2003). The volcanics from central Costa Rica have a restricted range in Zr/Nb ratios, indicating a more homogenous mantle source than the volcanics from modern northern Costa Rica. The central Costa Rica volcanics have been interpreted to be derived from a more enriched mantle source than those in northern Costa Rica due to the subduction of the Cocos Ridge in the proximity (Abratis and Worner, 2000; Herrstrom et al., 1995; Feigenson et al., 1996, 2004). While the Zr/Nb ratios of the modern arc

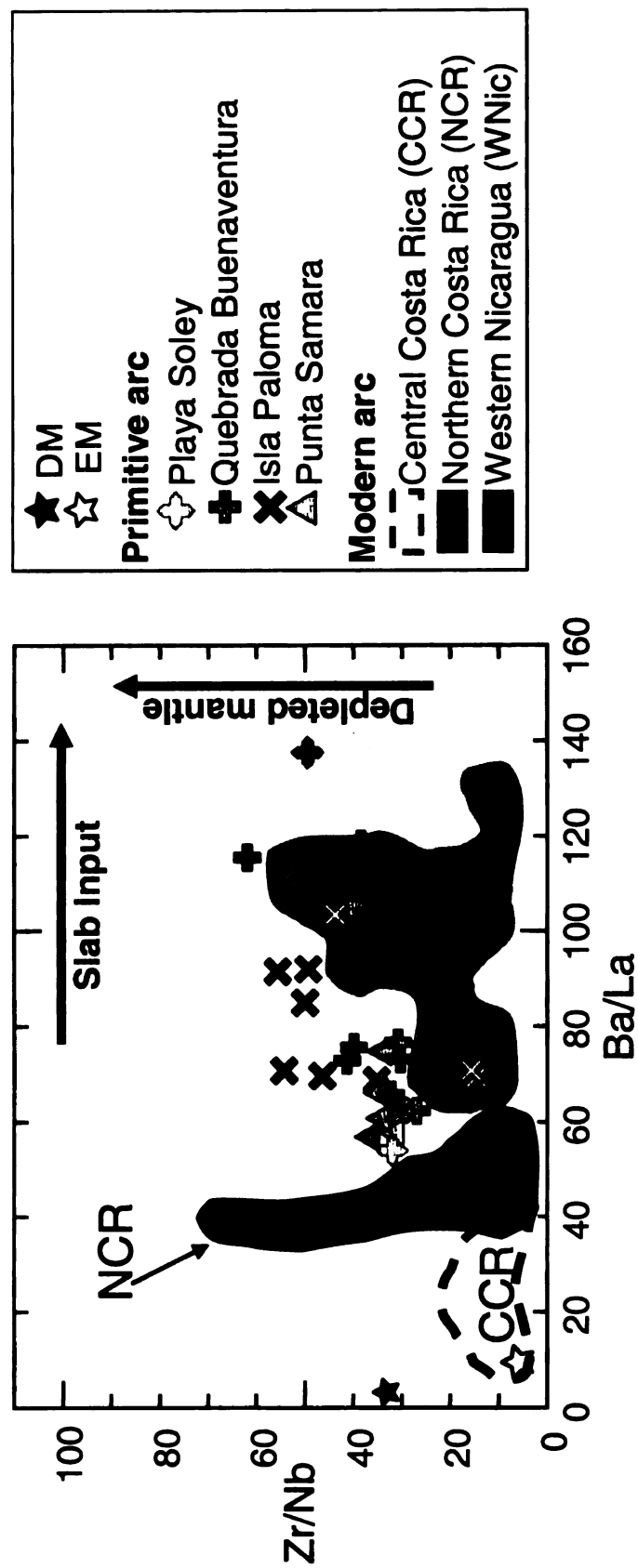


Figure 16. Volcanics with higher Zr/Nb ratios indicate a more depleted mantle source. Increasing Ba/La ratios indicate greater slab contribution to the lavas. DM and EM compositions are N-MORB and OIB, respectively, from Sun and McDonough, 1989.

volcanics from northern Costa Rica indicate that these originated from a heterogeneous mantle source composed of both an enriched (lower Zr/Nb) and a depleted (higher Zr/Nb) source (Abratis and Worner, 2000; Herrstrom et al., 1995; Feigenson et al., 1996, 2004). In northern Costa Rica, the volcanics are dominated by a depleted mantle source (Carr et al., 1990).

The primitive arc lava samples have a larger range of bulk rock compositions than the samples included in the above mentioned studies. However, the Zr/Nb ratio for the primitive arc lava samples does not correlate with SiO₂ (Figure 17). Therefore, fractional crystallization does not have an effect on the Zr/Nb ratio and can be used as a comparison for mantle source. The Zr/Nb ratio for the primitive arc volcaniclasts (15 to 62) overlaps the range of Zr/Nb ratios from the modern arc in northern Costa Rica (Figure 16). The two lavas from Isla Paloma, with the lowest Zr/Nb ratios from the primitive arc sample set, are similar to those from central Costa Rica. The samples from the primitive arc most likely originate from contributions from both a depleted and enriched mantle source, with the depleted source dominating.

Slab Signal

The slab signal in arc related lavas can be evaluated using trace element ratios as long as the ratio in the lavas is significantly different relative to that in mantle. Barium is highly mobile in hydrous fluids and La is considered immobile in these fluids (Pearce and Peate, 1995). The Ba/La ratio will be higher in arc volcanics due to fluids generated from the sediments and altered oceanic crust

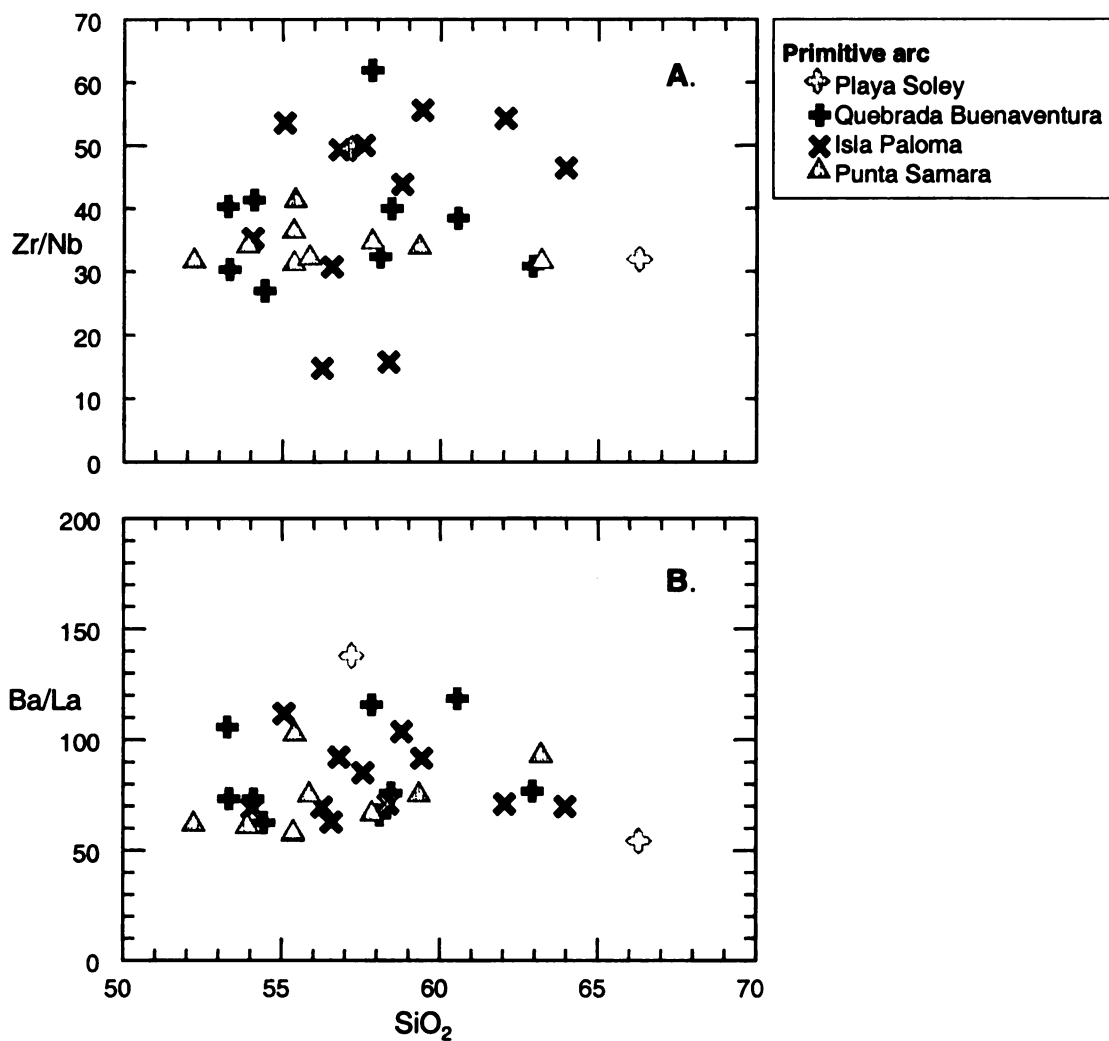


Figure 17. The Zr/Nb (A) and Ba/La ratios (B) of the lava samples are not correlated with SiO₂ (wt%).

from the subducting slab. For the modern Central American arc, Ba/La is considered an excellent geochemical tracer of slab signal from the Cocos Plate (Carr et al., 1990). The primitive arc lava samples have a larger range of bulk rock compositions than the samples included in the other studies mentioned. However, the Ba/La ratio for the primitive arc lava samples does not correlate with SiO₂ (Figure 17). Therefore, fractional crystallization does not have an effect on the Ba/La ratio and can be used as a comparison for slab signal.

The volcaniclasts from the primitive arc have Ba/La ratios higher than MORB or OIB (<15) (Figure 18). The lavas from Playa Soley have the widest range of Ba/La ratios for the primitive arc. The volcaniclasts from Quebrada Buenaventura separate into two groups based on the Ba/La ratios (greater than 100 or less than 80), while at Isla Paloma and Punta Samara, the lava samples have a continuous range of Ba/La ratios. For the modern arc in central Costa Rica, the Ba/La ratios (17 - 35) are lower than those from the primitive arc (Figure 18B). The primitive arc Ba/La ratios are mostly higher than those from the modern arc in northern Costa Rica (33-60). This indicates a generally higher slab contribution in the primitive arc than what is present in the modern arc in Costa Rica.

Carr et al. (1990) infer the degree of melting along the modern Central American volcanic arc using the variation of the slope of the REEs through La/Yb ratios. High La/Yb ratios indicate a lower degree of melting, and low La/Yb ratios indicate a higher degree of melting. The La/Yb values vary along the modern arc and the degree of melting correlates with the slab signal (Carr et al., 1990). The

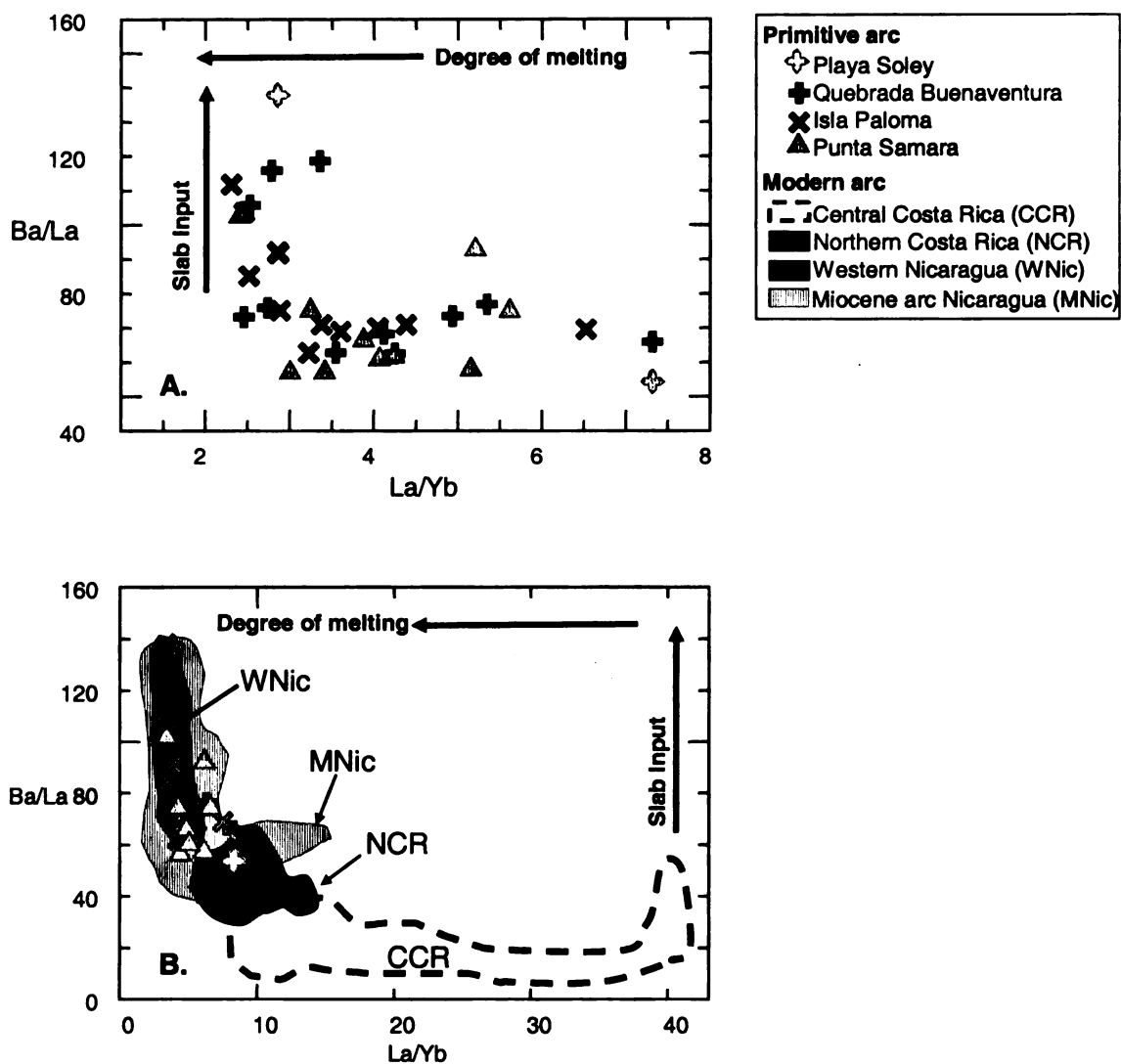


Figure 18. The Ba/La ratios from the volcanics from the primitive arc (A) show a correlation with the La/Yb ratio, similar to the modern arc volcanics (B).

highest slab signal and highest degree of mantle melting, based on Ba/La and La/Yb ratios, occurs in western Nicaragua, and decreases along the volcanic front away from this point. In the modern arc, in northern Costa Rica, the La/Yb values range from 6 to 12, and in central Costa Rica, the La/Yb values range from 7 to 38. The lower values for the slab tracers in the modern arc in Costa Rica, combined with higher La/Yb values indicates less slab input into the magmas, and a lower degree of mantle melting (Carr et al., 1990).

The correlation between degree of melting and slab signal is also present in the primitive arc, the higher Ba/La ratios generally correlate with lower La/Yb ratios (Figure 18A). The La/Yb ratios for the volcanoclasts from the primitive arc are lower than those from the modern arc in central Costa Rica. The primitive arc lavas have La/Yb ratios that are lower than, and overlap the lower range in La/Yb values for the modern arc in northern Costa Rica (Figure 18B). The higher Ba/La values and lower La/Yb values for the primitive arc can be interpreted to indicate that the primitive arc had a higher slab input and higher degree of mantle melting than the modern arc in Costa Rica. The lavas from the primitive arc display similar Ba/La and La/Yb ratios as what has been recorded from Miocene Nicaraguan and modern western Nicaraguan volcanics (Figure 18B).

For the modern Central American volcanic arc, Carr et al. (1990) proposed a model that links the regional variations in slab signal and degree of melting to the changes in the subduction angle of the Cocos Plate. In Nicaragua, the subduction angle is steeper and the angle shallows in Costa Rica. The steeper angle will produce metasomatism over a smaller volume of mantle resulting in a

greater degree of melting. The shallow angle will melt a greater volume of mantle, and it will melt to a lesser degree. Following this model, Patino et al. (2004) concluded the primitive arc in Costa Rica is presumed to originate from a steeper subduction angle than what is currently producing the modern arc in Costa Rica. The Farallon Plate must have been older, colder, and denser than the Cocos Plate in the region. Since the volcanics from the primitive arc have similar Ba/La and La/Yb ratios to those found in western Nicaragua, this study supports these conclusions.

Speculations on subducted sediment

Patino et al. (2000) characterized the geochemical changes in DSDP Site 495, a section on the Cocos Plate. The sediment package from the Cocos Plate, for the modern arc, consists of an underlying Middle to Lower Miocene carbonate sequence, approximately 200 meters thick, and an Upper Miocene to Quaternary hemipelagic sequence, 177 meters thick. These sediments are from the middle to lower Miocene, and upper Miocene-recent respectively. The change in sediment type is dated near 10 Ma, and represents the “carbonate crash” (Lyle et al., 1995). This occurred when the uplift of the Isthmus of Panama changed the eastern Pacific Ocean circulation pattern and elevated the carbonate compensation depth (Lyle et al., 1995). Each sediment type has a geochemical signature that is thus reflected in the slab signal.

Patino et al. (2000) found that the carbonate sediment section on the Cocos Plate has higher Ba/Th ratios than the hemipelagic section, and this ratio

is used as a tracer of the carbonate section in the modern Central American arc. Due to a greater abundance of organic matter in the hemipelagic sequence, the uranium concentrations are higher in the more recent sediments. Uranium is enriched over other elements and U/La and U/Th ratios are higher in the hemipelagic sediment section than the carbonate sediment section from the Cocos Plate (Patino et al., 2000).

The volcaniclasts from the primitive arc have Ba/Th ratios approximately between 308 and 1,530, except sample 040710-19 from Playa Soley that has a Ba/Th ratio of 2,907 (Figure 19A). The lavas from Punta Samara have the smallest range of Ba/Th ratios. The primitive arc lavas have higher Ba/Th ratios than those from central Costa Rica (~100 - 262), and have higher ratios or overlap the majority of the volcanics from northern Costa Rica (~296 - 808) (Figure 16). The volcanics from the modern arc in western Nicaragua have Ba/Th ratios (346 – 1,965) that are more similar to those from the primitive arc in Costa Rica (Figure 19).

The U/Th ratios for the primitive arc sample locations (Figure 20) are similar to the U/Th ratios present in the modern arc in central and northern Costa Rica (0.32 to 0.56), excluding the high U/Th ratios for the Playa Soley sample 040710-19 (Figure 20).

The modern arc volcanics from Costa Rica have lower U/Th ratios than those from the western Nicaraguan modern arc (0.67 - 0.97) (Carr et al., 2003). In modern Costa Rica, the lower geochemical sediment signatures have been attributed to underplating. This is a process where sediment is scraped off from

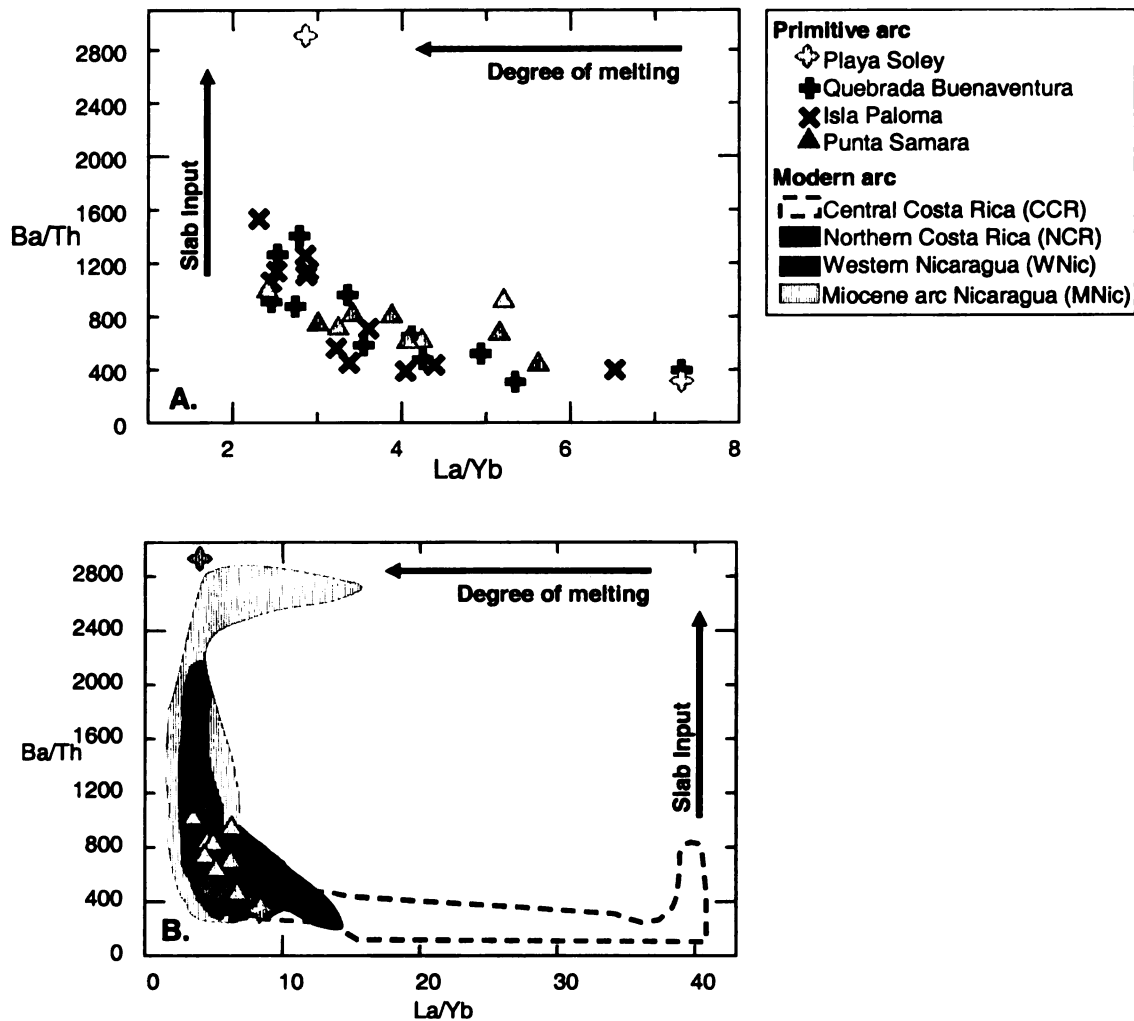


Figure 19. The Ba/Th variation for the primitive arc also decreases with an increase in La/Yb ratio (A). The primitive arc lava samples have Ba/Th ratios most similar to Miocene and modern western Nicaraguan volcanics (B).

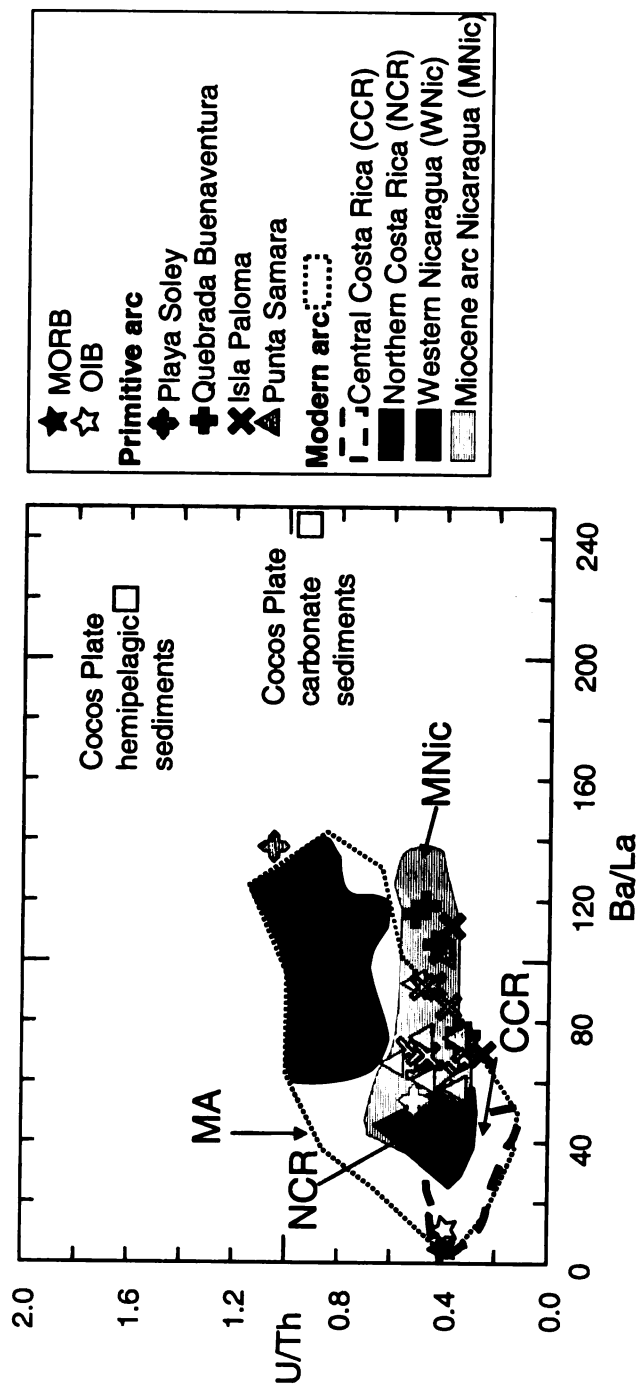


Figure 20. The primitive arc lava samples have U/Th ratios similar to those from Miocene Nicaragua and modern Costa Rica.

the downgoing slab, resulting in a lower sediment input into the arc lavas (Valentine et al., 1997). Although the primitive and modern arcs in Costa Rica have similar U/Th values, the processes that lead to these values are different. Patino et al. (2004) mention that in the primitive arc, the low U/Th ratios are most likely due to the absence of hemipelagic sediments in the sediment package. If underplating were the cause of the low U/Th ratios in the primitive arc lavas, the Ba/La ratios would also be lower, as is the case in the modern arc volcanics in Costa Rica. Given the high Ba/La ratios for primitive arc volcaniclasts, underplating is not the cause of the low U/Th ratios. The low U/Th ratios in the additional volcanics from the primitive arc, included in this study, support the conclusions of Patino et al. (2004). As Patino et al. (2004) also mentioned, a more likely explanation for the U/Th values in the primitive arc is that the hemipelagic sediments were absent from the subducting sediment package because they are older than the “carbonate crash”.

Plank et al. (2002) found that older lavas from Nicaragua (Early- Middle Miocene), also have lower U/Th values (0.38 – 0.60) than what is present in the more recent western Nicaraguan volcanics. The difference between U/Th values in volcanics from the Miocene and modern arcs in Nicaragua has been attributed to the absence of hemipelagic sediments contributing to the Miocene lavas because this occurred before the “carbonate crash”. While in the modern arc in western Nicaragua, which occurs after the “carbonate crash”, subducted hemipelagic sediments contribute to the magmas (Plank et al. 2002). The lavas from the primitive arc in Costa Rica have similar U/Th ratios as presented by

Plank et al. (2002) for Miocene Nicaraguan lavas (Figure 20). In addition, the Ba/Th ratios in the primitive arc correlate better with La/Yb ratios than the Ba/La ratios. If higher Ba/Th ratios and lower U is a signature of the carbonate section in the modern arc, then during the Paleogene carbonate sediments most likely dominated the sediment being subducted.

Conclusions

The primitive arc volcanoclasts from the four locations in Costa Rica (Punta Samara, Isla Paloma, Quebrada Buenaventura, and Playa Soley) range from basaltic to dacitic in composition. The primitive arc lavas included in the geochemical portion of the study are the result of subduction related magmatism, when the Farallon Plate subducted underneath the Caribbean Plate (Late Cretaceous to Eocene). Primitive arc magmas appear to be derived from a mixture of a depleted and enriched mantle, dominated by the depleted mantle component, similar to the modern arc in northern Costa Rica. However, two lavas from the primitive arc originate primarily from a more enriched mantle source, similar to what is observed in modern central Costa Rica. The slab input and degree of melting is higher for the primitive arc than the modern arc in Costa Rica, and more similar to what is present in the modern western Nicaraguan volcanics. This may be reflection an increased angle of subduction because the Farrallon Plate was older colder and denser than the Cocos Plate (Figure 21). The sediment subducted may have been similar to the carbonate sediment that is subducted in the modern arc. The primitive arc volcanoclasts lack the signature

of the hemipelagic sediment component present in the modern arc, comparable to the Miocene Nicaraguan volcanics.

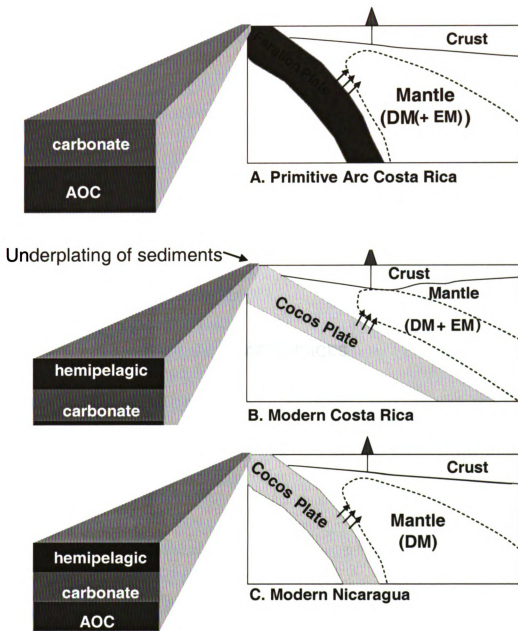


Figure 21. Comparison of the primitive arc in Costa Rica (A) to the modern arc in Costa Rica (B) and western Nicaragua (C). Diagram after Carr et al., 1990.

APPENDICES

APPENDIX A

Petrographic descriptions of altered samples.

Sample	Description
PA8	<p>Sample PA8 is a lava sample from Punta Samara. The phenocrysts comprise 60% of the sample. Subhedral plagioclase phenocrysts comprise 40% of the sample and are up to 2 mm in size. Plagioclase phenocrysts exhibit sericite. Plagioclase phenocrysts are partially altered to chlorite. Ten percent of the sample is comprised subhedral pyroxene grains are up to 3.5 mm in size and most are broken. Anhedral opaques comprise 5% of the sample and are most likely secondary and are up to 0.75 mm in size. Approximately 5% of the sample is comprised of phenocrysts replaced by calcite, chlorite, opaques and other alteration products. The groundmass comprises 55% of the sample. The groundmass consists of the phenocryst assemblage and previously mentioned alteration products. Calcite is also present in 10% of the groundmass.</p>
PA10	<p>Sample PA10 is a lava sample from Punta Samara. Phenocrysts comprise 45% of the section Subhedral plagioclase phenocrysts are present in 35% of the sample, and are up to mm in size. Plagioclase phenocrysts display sericite, alteration to chlorite. The pyroxene phenocrysts comprise less than 1% of the sample. The majority of pyroxene phenocrysts display reaction rims of opaques. Approximately 10% of the phenocrysts are completely altered to chlorite and possibly amphibole, and have reaction rims of opaques. The groundmass comprises 55% of the sample, and consists of 45% cryptocrystalline material, which appears to be the phenocryst assemblage in approximately the same proportions. Chlorite is present in approximately 10% of the groundmass. Fissures of calcite run across less than 1% of the section.</p>
PA19	<p>Sample PA19 is a sedimentary rock.</p>

Sample	Description
040709-19	<p>Sample 040709-19 is a lava sample from Isla Paloma. A large portion of this thin section is missing. The remaining portion of the section consists of 65% phenocrysts. Thirty-five percent of the phenocrysts are subhedral plagioclase that are up to 1.3 mm in length. Fifteen percent of the phenocrysts are euhedral pyroxene that are up to 0.6 mm in size. Approximately 15% of the phenocrysts have been completely altered to chlorite and calcite. Partial alteration to chlorite and calcite is also present on the phenocrysts. The groundmass comprises 35% of the section that is present and consists of smaller versions of the phenocrysts assemblage and alteration products and includes approximately 5% opaques.</p>
040709-26	<p>Is a lava sample from Isla Paloma. Phenocrysts compose 55% of the section. Approximately 35% of the phenocrysts are subhedral plagioclase that is up to 2.625 mm in length. Plagioclase phenocrysts display sericite and alteration to chlorite. Approximately 10% of the grains appear to be amphibole. Some of this amphibole may be secondary and display reaction rims. Less than 1% of the section is euhedral pyroxene phenocrysts up to 0.75 mm. Approximately 1% of the grains have altered to calcite. Transmineral fissures cross the section in a few areas. The groundmass is 45% of the sample. The groundmass is comprised of the 40% of the groundmass consists of the phenocryst assemblage and alteration products in approximately the same proportions and 5% is secondary opaques.</p>
040709-4	<p>This is a lava sample from Quebrada Buenaventura that was eliminated from the geochemical portion of the study due to a low total. The phenocrysts comprise 40% of the sample. Subhedral plagioclase phenocrysts comprise 25% of the sample and are up to 2.3 mm in length, The plagioclase phenocrysts display sericite and contain intramineral fissures. Fifteen percent of the phenocrysts are euhedral pyroxene that are up to 1.8 mm in length. Secondary opaques form reaction rims along pyroxene grains. The groundmass includes 55% of the sample. The groundmass is comprised of 20% calcite, 15% reddish brown material, 10% opaques, and 10% of the phenocryst assemblage.</p>

Sample	Description
040709-12	Sample 040709-12 is a basaltic trachyandesite from Quebrada Buenaventura. The sample is comprised of 55% phenocrysts. Thirty percent of the phenocrysts are subhedral plagioclase that display sericite, and are up to 2.5 mm in size. Calcite and chlorite are partially and completely replacing plagioclase grains. Ten percent of the phenocrysts are completely replaced by calcite. Ten percent of the phenocrysts are subhedral pyroxene that are up to 1.5 mm in size. Several of the grains are broken and secondary opaques have formed. Anhedral opaques are up to 0.5 mm in size and comprise 1% of the phenocrysts. The groundmass composes 50% of the sample and includes plagioclase, pyroxene, calcite, and opaques
17-5	Sample 17-5 is from Quebrada Buenaventura. The phenocrysts comprise 60% of the sample. Thirty-five percent are subhedral plagioclase phenocrysts that are up to 3 mm in length. Plagioclases exhibit sericite. Subhedral pyroxene phenocrysts comprise 15% of the section, are up to 1.3 mm. Secondary opaques have formed near pyroxene grains and are up to 0.5 mm. Approximately 10% of the phenocrysts have been completely replaced by calcite. Some phenocrysts have partially altered to chlorite. The groundmass is 40% of the section and contains cryptocrystalline material, opaques, calcite, and chlorite.
040710-12	Sample 040710-12 is a lava sample from Playa Soley. The phenocrysts comprise 5% of the section. Anhedral feldspar phenocrysts are up to 1.25 mm and comprise 5% of the section. The feldspar appear to have reaction rims along some grain boundaries. Less than 1% are anhedral quartz phenocrysts that are up to 0.8 mm. Less than 1% of the phenocrysts are anhedral opaques up to 0.5 mm. The groundmass is 95% of the sample and is composed of cryptocrystalline material.
040710-13	Sample 040710-13 is a fiamme sample from Playa Soley. The phenocrysts comprise 15% of the section. Anhedral feldspar phenocrysts are up to 2.25 mm and comprise 10% of the phenocrysts. The feldspar appear to have reaction rims along some grain boundaries. The remainder of the phenocrysts are opaques or grains that have been altered with a reddish brown material. The groundmass is 85% of the sample and is composed of cryptocrystalline material including reddish brown alteration products and opaques.

Sample	Description
040710-14	Sample 040710-14 is a lava sample from Playa Soley. The phenocrysts comprise 5% of the section. Anhedral feldspar phenocrysts are up to 1.3 mm and comprise 5% of the section. The feldspar appear to have reaction rims along some grain boundaries. Less than 1% are anhedral quartz phenocrysts that are up to 0.75 mm. Less than 1% of the phenocrysts are anhedral opaques up to 0.5 mm. The groundmass is 95% of the sample and is composed of cryptocrystalline material
040710-15	Sample 040710-15 is from Playa Soley. The phenocrysts comprise 15% of the section. Five percent are anhedral quartz phenocrysts that are up to 1.0 mm. Anhedral feldspar phenocrysts are up to 2.0 mm and comprise 5% of the section. Feldspar phenocrysts appear to have reaction rims along boundaries. Approximately 5% consists of opaques and grains that appear to have been replaced by opaques and alteration materials. The groundmass is 85% of the sample and is composed of cryptocrystalline material, opaques, and reddish brown alteration products.
040710-17	Sample 040710-17 is a lava sample from Playa Soley. The phenocrysts comprise 15% of the section. Five percent are anhedral quartz phenocrysts that are up to 1.5 mm. Anhedral feldspar phenocrysts are up to 2.5 mm and comprise 5% of the section. Approximately 5% consists of opaques and grains that appear to have been replaced by opaques and alteration materials. The groundmass is 85% of the sample and is composed of cryptocrystalline material.

Sample	Description
040710-18	<p>Sample 040710-18 is from Isla Paloma. This sample is composed of approximately 45% phenocrysts. Forty percent of the phenocrysts are subhedral plagioclase an up to 2.8 mm in length. The center of several plagioclase grains exhibit sericite and alteration to chlorite. Secondary opaques have also formed on some grains. Less than 1% of the phenocrysts have been completely replaced by calcite and chlorite. Five percent of the phenocrysts are replaced by alteration products and may have been pyroxene, and are up to 1.7 mm in size. Less than 1% of the sample contains quartz phenocrysts that are up to 0.8 mm in size. Resorption/reaction rims are present along most grain boundaries. The groundmass comprises 55% of the sample, and consists of 35% cryptocrystalline material, some of which may be the remnants of altered phenocrysts. Fifteen percent of the groundmass is opaques, along with 5% chlorite and reddish brown alteration.</p>
040710-20	<p>Sample 040710-20 is a fiamme sample from Playa Soley. The phenocrysts comprise 10% of the sample. Approximately 10% are subhedral feldspar phenocrysts that are up to 2.3 mm in size. Some feldspar phenocrysts contain fissures and display sericite. Less than 1% of the phenocrysts are anhedral quartz up to 1 mm in size. The groundmass comprises 90% of the sample. The groundmass is composed of cryptocrystalline material. In areas this material forms radial patterns. The groundmass has traces of a reddish brown material and opaques.</p>
040710-23	<p>Sample 040710-23 is a fiamme sample from Playa Soley. The phenocrysts comprise 5% of the sample. Approximately 5% are subhedral feldspar phenocrysts that are up to 1.7 mm in size. Some feldspar phenocrysts contain fissures, display sericite, and appear to be partially resorbed. Less than 1% of the phenocrysts appear to be replaced grains with opaques and reddish brown alteration, possibly oxyhornblende. The groundmass comprises 95% of the sample. The groundmass is composed of cryptocrystalline material. The groundmass has traces of a reddish brown material and opaques.</p>

Sample	Description
040710-24	Sample 040710-24 is a fiamme sample from Playa Soley. The phenocrysts comprise 5% of the sample. Approximately 5% are subhedral feldspar phenocrysts that are up to 1.8 mm in size. Some feldspar phenocrysts contain fissures, display sericite, and appear to be partially resorbed. Reaction rims appear around phenocrysts. The groundmass comprises 95% of the sample. The groundmass is composed of cryptocrystalline material. The groundmass has traces of a reddish brown material and opaques. In areas this appears in a radial pattern.
031024-4a	Sample 031024-4a is a fiamme sample from Playa Soley. The phenocrysts comprise 5% of the sample. Approximately 5% are subhedral feldspar phenocrysts that are up to 2.3 mm in size. Some feldspar phenocrysts contain fissures, display sericite, and appear to be partially resorbed. Approximately 2% of the phenocrysts have altered to chlorite. Less than 1% of the phenocrysts appear to be replaced grains with opaques. The groundmass comprises 95% of the sample. The groundmass is composed of cryptocrystalline material. The groundmass has traces of a chlorite, reddish brown material, and opaques.
031024-4b	Sample 031024-4b is a fiamme sample from Playa Soley. The sample contains approximately 5% phenocrysts of anhedral feldspar that are up to 1.3 mm in size. The groundmass is comprised of cryptocrystalline material that may be altered glass and opaques.
031024-4c	Sample 031024-4c is a fiamme sample from Playa Soley. The sample contains approximately 5% phenocrysts of anhedral feldspar that are up to 1.5 mm in size. Approximately 5% of the phenocrysts are grains that have been replaced by opaques and reddish brown alteration products. Ninety percent of the section is groundmass. The groundmass is comprised of cryptocrystalline material that may be altered glass and opaques
031024-4d	Sample 031224-4d is a fiamme sample from Playa Soley. The phenocrysts comprise 20% of the sample. Fifteen percent of the phenocrysts are anhedral feldspar grains that are up to 2.25 mm in length. Five percent of the phenocrysts are anhedral quartz that are up to 1.5 mm. The groundmass comprises 75% of the section. It contains cryptocrystalline material and opaques.

Sample	Description
031024-4e	Sample 031024-4e is a fiamme sample from Playa Soley. The phenocrysts comprise 15% of the section. Approximately 10% of sample is anhedral feldspar up to 1.3 mm. The remaining 5% of the phenocrysts consists of anhedral quartz phenocrysts that are up to 1mm in size, and anhedral opaques that are up to 0.5 mm in size. The groundmass comprises 85% of the sample, and consists of 80% cryptocrystalline material, and 5% of the remnants of altered phenocrysts that have been disaggregated and secondary opaques.
031024-4f	Sample 031024-4f is a fiamme sample from Playa Soley. The phenocrysts comprise 15% of the sample. Approximately 10% of sample is anhedral feldspar up to 1.5 mm. The remaining phenocrysts appear to be phenocrysts that have been replaced by reddish brown alteration and opaques. The groundmass is 85% of the section and consists of cryptocrystalline material that may be altered glass.
031024-4g	Sample 031024-4g is a fiamme sample from Playa Soley. Ten percent of the sample is comprised of phenocrysts. Anhedral feldspar phenocrysts are up to 1.3 mm in size. Less than 1% of the phenocrysts are anhedral quartz that are up to 1 mm in size. The groundmass comprises 90% of the sample, and consists of cryptocrystalline material and opaques.
031024-4h	Sample 031024-4h is a fiamme sample from Playa Soley. Phenocrysts are present in 15% of the sample. Anhedral feldspar comprises 10% of the phenocrysts, and are up to 1.5 mm in size. Anhedral quartz phenocrysts comprise 5% of the sample and are up to 1.8 mm in size. Grains that have been replaced by opaques and reddish brown alteration comprise less than 1% of the section. The groundmass consists of cryptocrystalline material and opaques.
031024-4i	Sample 031024-4i is a fiamme sample from Playa Soley. The phenocrysts comprise 10% of the sample, and are anhedral feldspar up to 1.3 mm in size. The groundmass is 90% of the section and consists of cryptocrystalline material that may be altered glass.

Sample	Description
PD1-21-0202	Sample PD1-21-0202 is a lava sample from Playa Rajada, and consists of 5% phenocrysts that are primarily anhedral feldspar that are cracked and have reaction rims. The feldspar are up to 1.5 mm in size. The sample contains less than 1% of grains that have been replaced by opaques and reddish brown material. These replaced grains are up to 0.3 mm in size. The groundmass comprises 95% of the section and is cryptocrystalline material.
PD3-21-0202	Sample PD3-21-0202 is a lava sample from Playa Rajada, and consists of 100% groundmass. The groundmass is composed of reddish brown material and opaques. There almost appears to be a pattern similar to flow banding of opaques in areas. Less than 1% of the sample appears to be grains that have been replaced or altered with opaque and reddish brown material.

APPENDIX B

Minerals present in thin sections

Table 4. Minerals present in thin section.

Phen % is percentage of phenocrysts present in the section. Plag is plagioclase, Pyx is Pyroxene, Opq is opaques, Qtz is quartz, Amph is amphibole, Cal is calcite, and Chl is chlorite. * is feldspar in the sample that is most likely plagioclase.

Sample	Phen %	Plag	Pyx	Opq	Qtz	Amph	Cal	Chl
PA 040709-1	40	X	X	X			X	X
PA 040709-2	65	X	X	X			X	X
PA 040709-3	65	X	X	X			X	X
PA 040709-4	40	X	X	X			X	
PA 040709-5	40	X	X	X				X
PA 040709-6	35	X	X	X			X	X
PA 040709-9	40	X	X	X			X	X
PA 040709-10	65	X	X	X			X	X
PA 040709-12	55	X	X	X			X	X
PA 040709-13	55	X		X			X	X
PA 040709-14	15	X		X	X			
17-5-1201	60	X	X	X			X	X
PA 040709-15	55	X	X	X				
PA 040709-16	55	X	X	X				
PA 040709-17	65	X	X	X				X
PA 040709-18	65	X	X	X				X
PA 040709-19	65	X	X				X	X
PA 040709-20	40	X	X	X				X
PA 040709-21	60	X	X	X			X	X
PA 040709-22	55	X	X	X			X	X
PA 040709-24	40	X	X	X		X		X
PA 040709-25	50	X	X	X				X
PA 040709-26	35	X	X	X		X	X	
14-11-1201	40	X	X	X			X	X
13-11-1201	35	X	X	X			X	X
PA 040710-12*	5	X		X	X			
PA 040710-14*	5	X		X	X			
PA 040710-15*	15	X		X	X			
PA 040710-16	40	X		X			X	X
PA 040710-17*	15	X		X	X			
PA 040710-18	45	X	X	X			X	X
PA 040710-19	50	X		X			X	X
PA 040710-20*	10	X			X			
PA 040710-23*	5	X		X		X		
031024-4a*	5	X		X				X
031024-4b*	5	X		X				
031024-4c*	5	X		X				
031024-4d*	20	X		X	X			
031024-4e*	15	X		X	X			
031024-4f*	15	X		X				
031024-4g*	10	X		X	X			
031024-4h*	15	X		X	X			
031024-4i*	10	X						
PD3-21-0202	0			X				

Table 4 (continued)

Sample	Phen %	Plag	Pyx	Opq	Qtz	Amph	Cal	Chl
PD1-21-0202*	5	X		X				
PA5	55	X	X	X				
PA6	45	X	X	X			X	
PA8	60	X	X	X			X	X
PA9	55	X	X	X				
PA10	45	X	X	X		X	X	X
PA11	50	X	X	X			X	
PA12	45	X	X	X			X	
PA13	65	X	X	X			X	
PA14	45	X		X			X	X
PA15	35	X		X			X	X
PA18	35	X	X	X				X

APPENDIX C

Anomalous Slab Signal (Ce/Pb)

Anomalous Slab Signal

The samples from the primitive arc in Costa Rica have Ce/Pb ratios that range from 5 to 39 (Figure 22). According to Noll et al. (1986) arc related magmas have Ce/Pb ratios between 1 and 10. In MORB and OIB, Ce/Pb ratios are greater than 20, according to Hoffman et al. (1988), and near 25 according to Sun and McDonough (1989). Both Pb and Ce have similar incompatibility in mantle minerals, therefore, during melting these two elements should not be fractionated. The characteristic Ce/Pb range of arc lavas has been explained by the preferential extraction of Pb over Ce by fluids from the subducting oceanic crust, resulting in a lower Ce/Pb ratio in arc magmas than what is present in MORB or OIB (Miller et al., 1994; Brennan et al., 1995). Researchers have also suggested that Ba and Pb behave similarly in subduction zone related magmatism (e.g., Shibata and Nakamura, 1997). Lead has also been reported to be more mobile than other LILE in fluids that are produced by the dehydration of amphibolite (Kogiso et al., 1997). Therefore, if a high slab contribution is present and Ba/La ratios are high, Ce/Pb ratios would be expected to be low.

Five of the primitive arc lavas have Ce/Pb ratios greater than 14 (Figure 23) due to lower Pb concentrations in the samples. However, a high slab contribution is still evident in these lavas ($Ba/La > 50$) (Figure 22). The volcanics from the modern arc in Central America have Ce/Pb ratios that range from <1 to 31 (Figure 22 and 23). However, the majority of the modern arc volcanics have Ce/Pb ratios that are 14 or less. The higher range of Ce/Pb ratios (>14) from the modern arc occur in central Costa Rican volcanics. The volcanics from central

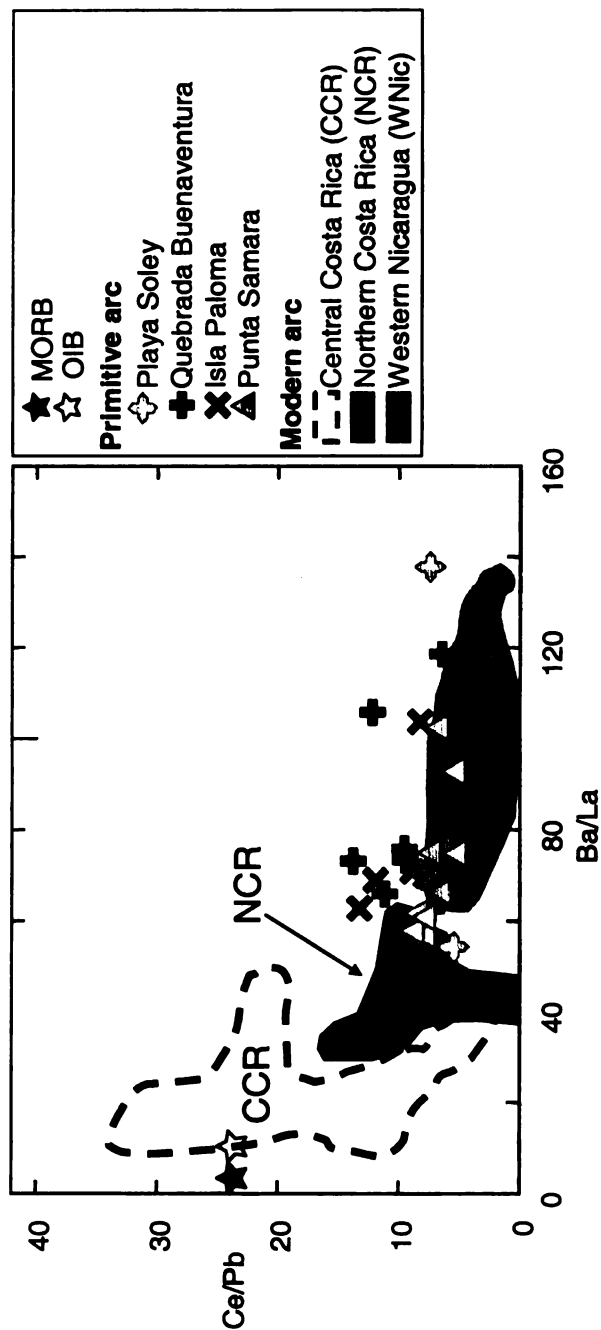


Figure 22. Some lava samples from the primitive arc have high Ce/Pb ratios and high Ba/La ratios (>50). Samples from the primitive arc with Ce/Pb ratios >14 are shown as open symbols. OIB and MORB are from Sun and McDonaugh, 1989.

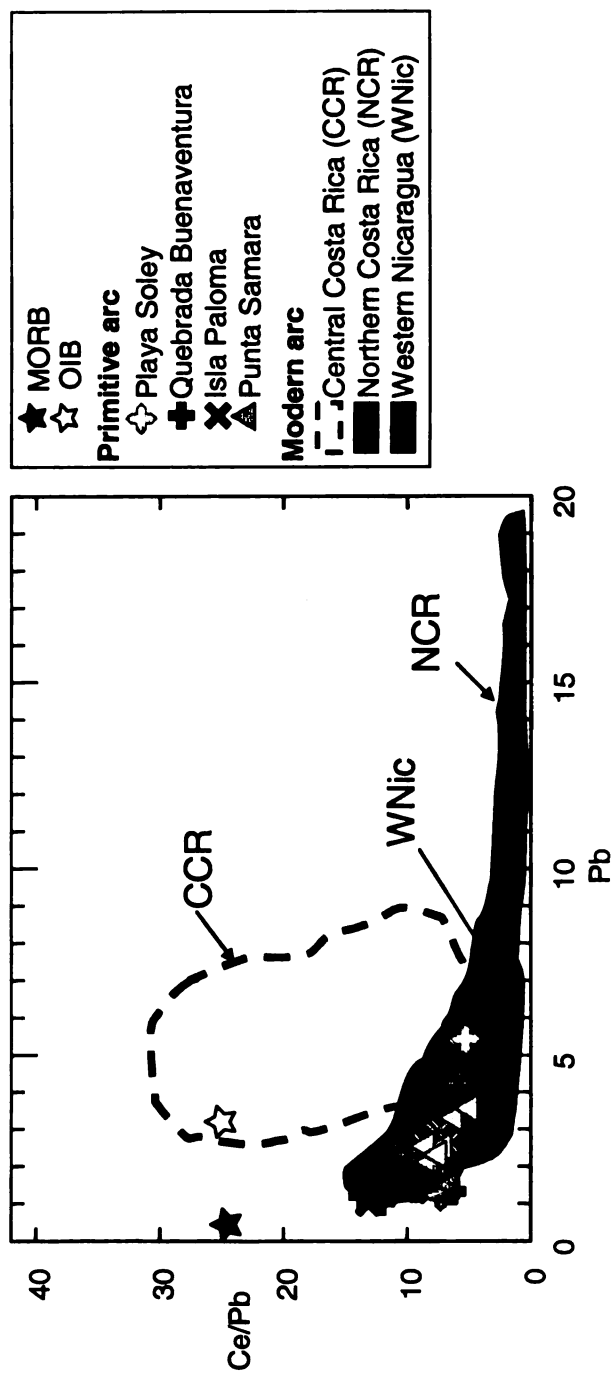


Figure 23. The lava samples with high Ce/Pb ratios from the primitive arc (open symbols) are due to low Pb concentrations in the samples. MORB and OIB are from Sun and McDonaugh, 1989.

Costa Rica with high Ce/Pb differ from those from primitive arc in that modern lavas do not have as high of a slab contribution ($Ba/La < 50$) (Figure 22).

One explanation for the low-Pb samples from the primitive arc is analytical error. Lead is highly volatile and it can be lost during fusion of the samples/and or during ablation. In addition, different sample matrices couple differently with the laser during ablation. However, these samples were all fused for the same amount of time as other samples with high Pb concentrations; therefore, any Pb loss should be uniform. Also, the low-Pb lavas have similar major element concentrations to the rest of the samples, with the exception of K_2O , which is low among these samples. However, there are other lavas that have higher Pb values and still have similar K_2O contents. All of the low-Pb samples have $SiO_2 < 70$ wt% and were ablated as long as other samples with similar SiO_2 content. There appears to be no correlation between the low-Pb samples and ablation time. In addition, these samples were all analyzed in the LA ICP-MS on the same day using the same regression lines to calculate the results.

Another explanation for the low Pb samples from the primitive arc is that these volcanics are not arc related. Hoffman (1988) compiled an average for the Pb concentrations in N-MORB (0.489 ppm) and continental crust (8.0 ppm). In addition, Sun and McDonough (1989) compiled the Pb concentrations in N-MORB (0.30 ppm), E-MORB (0.60 ppm), and OIB (3.20 ppm). The primitive arc Pb concentrations range from 0.27 to 5.44 ppm, and in the low-Pb samples the concentration ranges from 0.27 to 0.80 ppm. The Pb concentrations from the modern arc range from approximately 1.8 to 19 ppm, with the majority between 2

and 11 ppm. Other than the low Pb concentrations, the low-Pb samples from the primitive arc have the chemical characteristics of subduction zone related lavas, displaying enrichment of LILE over HFSE (Figure 24).

A third explanation for the low-Pb from the primitive arc samples is that the slab contribution varied in these lavas. Patino et al. (2000) proposed a flux model for the modern arc in Central America. The influx portion of the model includes the hemipelagic sediment, carbonate sediment, and altered oceanic crust. As previously discussed, it is unlikely that a hemipelagic sediment component contributes to the primitive arc lavas. However, it is possible that a carbonate sediment component and altered oceanic crust contribute to the generation of the primitive arc volcanoclasts. To estimate the contribution from the subducting oceanic crust in the modern arc, Patino et al. (2000) used DSDP Site 504B. Site 504B is dated at 7 Ma, and is 2 km in depth (Alt et al., 1996). This site consists of an upper volcanic section that has been oxidized and enriched in alkalis from the interaction with sea water. It is important to note that the upper section of oceanic crust is enriched in Rb, K, and U (Alt and other, 1996; Staudigel et al., 1995). In the middle is a transition zone that has been hydrothermally altered, and is enriched in chalcophile elements, including Pb, which have been leached from the lower hydrothermally altered dikes (Alt et al., 1996). Chauvel et al. (1995) and Alt et al. (1996) suggest that hydrothermal alteration in the oceanic crust promotes the deposition of sulfide minerals in the transition zone, thus adjusting the Pb content of the oceanic crust. In the modern arc, Patino et al. (2000) found that B, Rb, Cs, and K are contributed from the

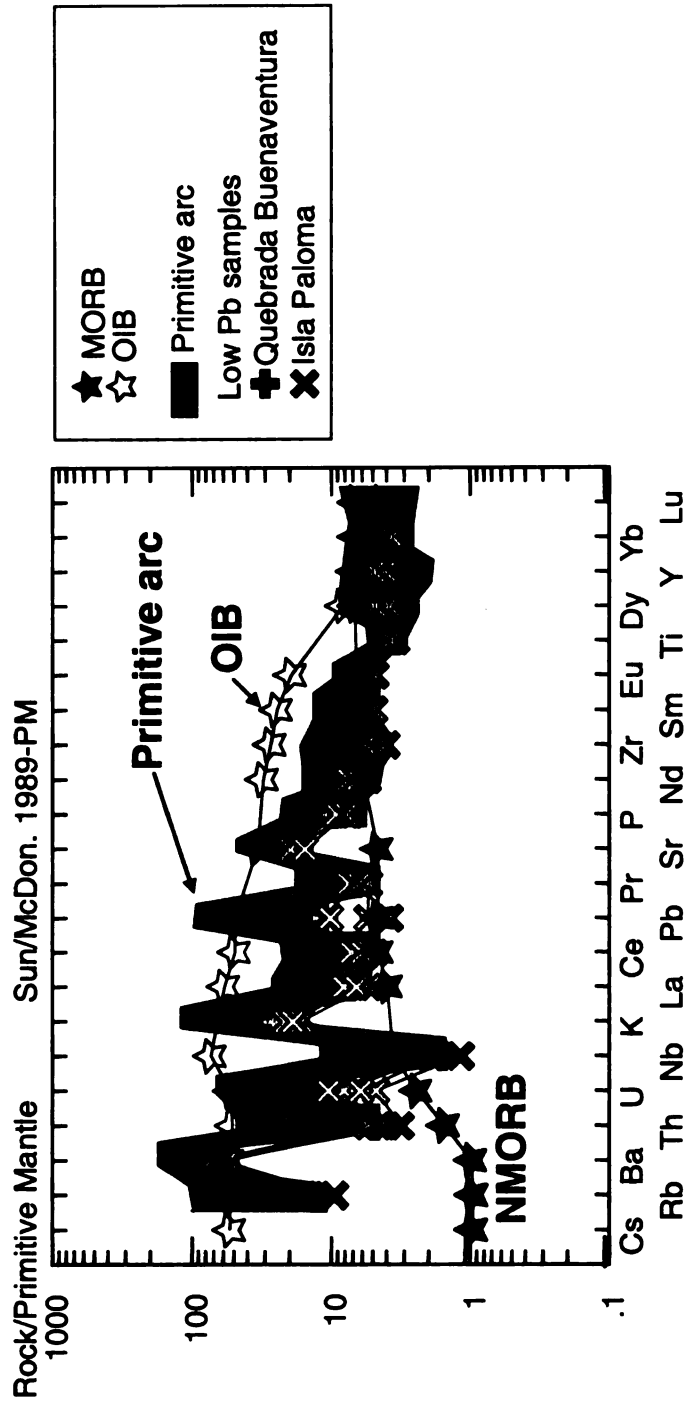


Figure 24. The low-Pb lava samples have the characteristics of arc related magmatism. OIB and MORB are from Sun and McDonough, 1989.

upper segment of the AOC, while the majority of the Pb is contributed from the hydrothermally altered portion of the AOC. Thorium and U are also contributed from the AOC. The data set from the primitive arc does not include B and Cs, however, in the low-Pb samples from the primitive arc Rb, K, U, and Th are near the lower range of values observed (Figure 25). It is possible that the low-Pb samples had a lower contribution from the AOC than the other primitive arc samples.

There are of course several uncertainties with this third hypothesis. Although the Rb, K, U, and Th concentrations for the low-Pb samples are amongst the lowest from the primitive arc, there are other lavas from the primitive arc that have similar values and do not have low-Pb concentrations. In addition, the Pb concentrations presented by Alt et al. (1996) are not well constrained due to contamination. Although close in geographic proximity to Central America, Site 504 is also younger than the primitive arc. Kelley et al. (2003) determined the chemistry of oceanic crust from ODP site 801, which is dated near 179 Ma, and is located in the western Pacific. The authors found that the oceanic crust at this site was enriched in U, K, Rb, along with Li and Cs, but did not find high Pb concentrations. Although the oceanic crust from ODP Site 801 is closer in age to the primitive arc, it is geographically farther away than the locality of the primitive arc, and is shallower (total of 470 m) than Site 504.

Due to the location and age of the samples, there is also the possibility that secondary processes may have removed elements from the lavas, resulting in the low-Pb primitive arc lavas. Noll et al. (1995) proposed that a reducing, acidic

hydrothermal fluid may preferentially mobilize chalcophile elements such as Pb over LILE, due to the presence of sulfides and other complexes. A sulfide rich hydrothermal fluid could have removed the Pb from the low-Pb lavas, and not mobilized as much Ba, not altering the Ba/La ratio in these samples.

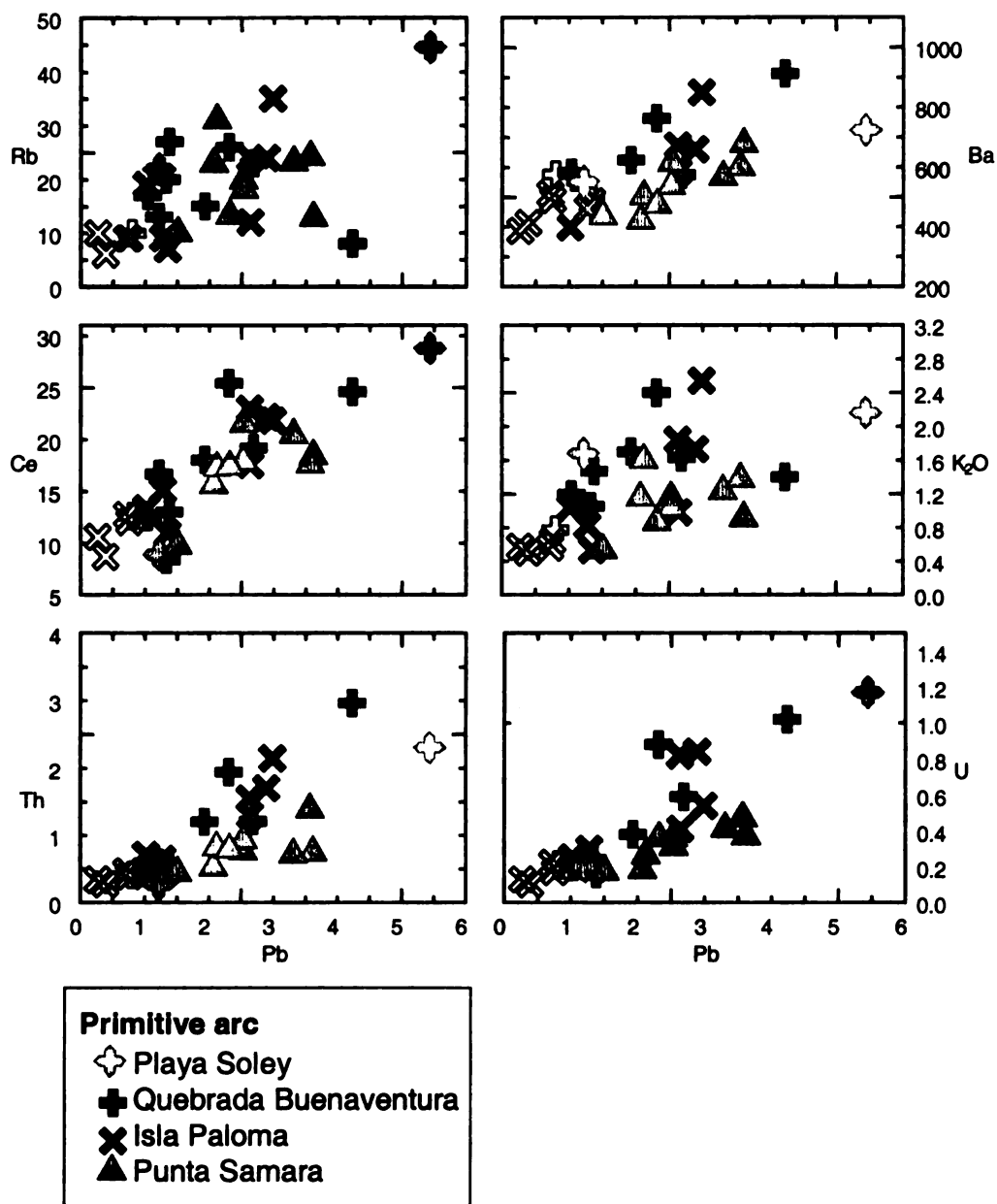


Figure 25. Selected elements versus Pb. Notice that the low-Pb samples (open symbols) also have low K₂O (wt%), Rb, Th, and U (ppm) compared to other primitive arc lava samples. However, the low-Pb samples do not have the lowest concentrations of Ce and Ba (ppm).

REFERENCES

- Abratis M., Worner, G., 2000. Ridge collision, slab-window formation, and the flux of Pacific aesthenosphere into the Caribbean realm. *Geology* 29, 127-130.
- Alt JC, Laverne C, Vanko DA, Tartarotti P, Teagle DAH, Bach W, Zuleger E, Erzinger J, Honnorez J, Pezard PA, Becker K, Salisbury MH, Wilkens RH (1996) Hydrothermal alteration of section of upper oceanic crust in the eastern equatorial Pacific: a synthesis of results from site 504 (DSDP legs 69, 70, and 83, and odd legs 111, 137, 140, and 148). *Proc ODP, Scientific Results* 148: 417-433.
- Astorga, AG, 1987. El Cretacico superior y el Paleogeno de la vertiente pacifica de Nicaragua meridional y Costa Rica septentrional: origin, evolucion dinamica de las cuencas profundas relacionadas al margen covergente de Centroamerica. Tesis de Grado. Universidad de Costa Rica.
- Ballance, PF, 1991. Gravity flows and rock recycling on the Tonga landward trench slope: relation to trench-slope tectonic processes. *Journal of Geology* 99: 817-827.
- Barckhausen, U, Ranero, C, von Huene, R, Cande, SC, Roeser, HA, 2001. Revised tectonic boundaries in the Cocos Plate off Costa Rica: Implications for the segmentation of the convergent margin and for plate tectonic models. *Journal of Geophysical Research* 106: 19207-19220.
- Baumgartner, PO, Mora, CR, Butterlin, J, Signal J, Glacon, G, Azema, J, Bourgois, J, 1984. Sedimentacion y paleogeografia del Cretacico y Cenozoico del litoral pacifico de Costa Rica. *Revista Geologica de America Central*
- Bourgois, J., Azema, J, Baumgartner, PO, Tournon, J, Desmet, A, Aubouin, J, 1984. The geologic history of the the Caribbean-Cocos plate boundary with special reference to the Nicoya Ophiolitic Complex and DSDP results (Leg 67 and 84 off Guatemala): a synthesis. *Tectonophysics* 108: 1-32.
- Brenan JM, Shaw HF, Ryerson FJ, 1995. Experimental evidence for the origin of lead enrichment in convergent-margin magmas. *Nature* 378: 54-56.
- Calvo, C, 2003. Provenance of plutonic detritus in cover sandstones of Nicoya Complex, Costa Rica: Cretaceous unroofing history of a Mesozoic ophiolite sequence *Geological Society of America Bulletin*: 115: 832-844.

- Calvo, C and Bolz, A, 1994. Der älteste kalkalkaline Inselbogen-Vulkanismus in Costa Rica: Marine pyroklastika der Formation Loma Chumico (Alb bis Campan). *Profil*, 7: 235-264.
- Carr, MJ, Feigenson, MD, Bennett, EA, 1990. Incompatible element and isotopic evidence for tectonic control of source mixing and melt extraction along the Central American arc. *Contributions to Mineralogy and Petrology* 105: 369-380.
- Carr, MJ, Feigenson, MD, Patino, LC, Walker, JA, 2003. Volcanism and geochemistry in Central America: progress and problems. *Geophysical Monograph* 138: 153-174.
- Chauvel C, Goldstein SL, Hofmann AW, 1995. Hydration and dehydration of oceanic crust controls Pb evolution in the mantle. *Chemical Geology* 126: 65-75
- Criss, JW, 1980. Fundamental Parameters calculations on a laboratory microcomputer. *Advances in X-ray Analysis* 23: 93-97.
- Dickinson, WR, 1985. Interpreting provenance relations from detrital modes of sandstones. In: Zuffa, G.G. (Ed.), *Provenance of Arenites*. Reidel Publ., Dordrecht, pp. 333–361
- Feigenson, MD, Carr MJ, 1993. The Source of Central American lavas: inferences from geochemical inverse modeling. *Contributions to Mineralogy and Petrology* 113: 226-235.
- Feigenson MD, Carr MJ, Patino L, Maharaj S, Juliano S, 1996. Isotopic identification of distinct mantle domains beneath Central America. *Abstracts with Programs, Geological Society of America* 28(7):380.
- Feigenson, MD, Carr, MJ, Maharaj, SV, Juliano, S, Bolge, LL, 2004. Lead isotope composition of Central American volcanoes: Influence of the Galapagos. plume, *Geochemistry, Geophysics, Geosystems*:10.1029/2003GC000621.
- Flores, KR, 2003. Propuesta tectonoestratigrafica de la region septentrional del Golfo de Nicoya, Coata Rica. *Univeridad de Costa Rica*. 176p.
- Gill, J, Hiscott, R, Vidal, Ph, 1994 1994 Turbidite geochemistry and the evolution of island arcs and of continents. *Lithos* 33, 135-168.
- Hauff, F, Hoernle, K, van der Bogaard, P, 2000. Age and geochemistry of basaltic complexes in western Costa Rica: contributions to the geotectonic

- evolution of Central America. *Geochemistry, Geophysics, Geosystems* 1: 999GC000020.
- Herrstrom EA, Reagan, MK, Morris, JD, 1995. Variation in lava compositions associated flow of aesthenosphere beneath Southern Central America. *Geology* 23:617-620.
- Hey, R, 1977. Tectonic evolution of the Cocos-Nazca spreading center. *Geological Society of America Bulletin* 88: 1404-1420.
- Hoernle, K, Van den Bogaard, P, Worner, R, Lissinna, B, Hauff, F, Alvarado, GE, Garbe-Schonberg, D, 2002. Missing History (16-71 Ma) of the Galapagos hotspot: implications for the tectonic and biological evolution of the Americas. *Geology* 30(9): 795-798.
- Hoffman, AW, 1988. Chemical differentiation of the earth: the relationship between mantle, continental crust, and oceanic crust. *Earth and Planetary Science Letters*, 90:297-314.
- Kelley, KA, Plank, T, Ludden, JN, STaudige, H, 2003. Composition of altered oceanic crust at ODP Sites 801 and 1149, *Geochem., Geophys. Geosyst.* 4 :10.1029/2002GC000435.
- Kogiso T, Tatsumi Y, Nakano S, 1997. Trace element transport during dehydration processes in the subducted oceanic crust: 1. Experiments and implications for the origin of ocean island basalts. *Earth and Planetary Science Letters* 148: 193-205.
- Kuijpers, EP, 1979. La geologica del Complejo Ophiolitico de Nicoya, Costa Rica. *Inf. Sem. Inst. Geogr. Nac.* 25:15-75.
- Lew, LR, 1983. The geology of the Osa Peninsula, Costa Rica: observations and speculations about the evolution of part of the outer arc of southern Central America. *orogen. Penn State University M.S. Thesis.* 128p.
- Lissinna, B, Hoernle, K, Van der Bogaard, P. 2002. Northern migration of arc volcanism in western panama: evidence for subduction erosion? AGU Fall Meeting, San Francisco, *EOS Trans* 83: V11A-1368.
- Lyle, M, Dadey, KA, Farrell, JW, 1995. The late Miocene (11-8 Ma) eastern Pacific carbonate crash: evidence of reorganization of deep-water circulation by closure of the Panama gateway, in Pisias, NG, Mayer, LA et al. *Proceedings of the Ocean Drilling Program, Scientific results*, 138:821-838.

- Lytwyn, J, Rutherford, E, Burke, K, XIA, C. 2001. The geochemistry of volcanic, plutonic and turbiditic rocks from Sumba, Indonesia. *Journal of Asian Earth Science* 19: 481-500.
- Maury, RC, Defant, MJ, Bellon, H, de Boer, JZ, Stewart, RH, Cotton, J, 1995. Early Tertiary arc volcanics from eastern Panama in Mann, P. ed., Geologic and Tectonic Development of the Caribbean Plate Boundary in Central America. Boulder, CO, GSA Special Paper 295: 29-34.
- Miller DM, Goldstein SL, Langmuir CH, 1994. Cerium/lead and lead isotope ratios in arc magmas and the enrichment of lead in the continents. *Nature* 368: 514-520.
- Parker, A, 1970. An index of weathering for silicate rocks. *Geological Magazine* 107: 501-504.
- Patino, LC, Carr, MJ, Feigenson, MD, 2000. Local and regional variations in Central American arc lavas controlled by variations in subducted sediment input. *Contributions to Mineralogy and Petrology* 138: 265-283.
- Patino, LC, Velbel, MA, Price, JR, Wade, JA, 2003. Trace element mobility during spheroidal weathering of basalts and andesites in Hawaii and Guatemala. *Chemical Geology* 202: 343-364.
- Patino, LC, Alvarado, GE, Vogel, TA, 2004. Early arc magmatism: geochemical characteristics of volcanic clasts from Punta Samara, Costa Rica. *Revista Geologica de America Central*, 30: 117-124.
- Noll, PD Jr., Newsom, HE, Leeman, WP, Ryan, JG, 1986. The role of hydrothermal fluids in the production of subduction zone magmas: Evidence from siderophile and chalcophile trace elements and boron. *Geochimica et Cosmochimica Acta* 60:587-611.
- Pearce, JA and Peate, DW, 1995. Tectonic Implications of the composition of volcanic arc magmas. *Annu. Rev. Earth Planet. Sci.* 1995. 23:251-85
- Pindell JL and Barrett SF, 1990. Geologic evolution of the Caribbean region: A plate tectonic perspective. In Dengo, G and Case JE (eds.): *The Geology of North America, The Caribbean region* H: 405-432.
- Plank, T, Balzer, V, Carr, MJ, 2002. Nicaraguan volcanoes record paleogeographic changes accompanying closure of the Panama gateway. *Geology* 30: 1087-1090.

- Rivier, F, 1983. Síntesis geológica y mapa geológico del área de bajo Tempisque, Guanacaste, Costa Rica.- Inf. Sem. I.G.N. 1983(1):7-30.
- Saito, S., 1998. Major and trace element geochemistry of sediments from East Greenland Continental Rise: an implication for sediment provenance and source area weathering. In Saunders, A.D., Larsen, H.C., and Wise, S.W., Jr. (Eds.), Proc. ODP, Sci. Results, 152: College Station, TX (Ocean Drilling Program), 19-28.
- Schott, R.C. and Johnson, C.M., 1998, Sedimentary record of the Late Cretaceous thrusting of the Salina-Mohave magmatic arc. *Geology* 26, 327-330.
- Shibata T, Nakamura E, 1997. Across-arc variations of isotope and trace element compositions from Quaternary basaltic volcanic rocks in northeastern Japan: implications for interaction between subducted slab and mantle wedge. *J Geophysical Research* 102:8051-8064.
- Staudigel H, Davies GR, Hart SR, Marchant KM, Smith BM, 1995. Large scale isotopic Sr, Nd and O isotopic anatomy of altered oceanic crust: DSDP/ODP sites 417/418. *Earth Planet Sci Lett* 130: 169-185.
- Sun S, McDonough WF, 1989. Chemical and isotopic systematics of oceanic basalts: implications for mantle composition and processes. In: Saunders AD, Norroy MJ (eds) *Magmatism in the ocean basins*. *Geol Soc Spec Publ* 42: 313-345.
- Tournon, J, 1984. Magmatismes du Mesozoic a l'actuel en Amerique Central: L'exemple de Costa Rica, des ophiolites aux andesites. *Memoires Sciences Terre, Univ. Pierre Marie Curie Ph. D. Thesis*. 335p.
- Valentine RB, Morris JD, Duncan D, Jr., 1997. O.S.P.L. 170, Sediment subduction, accretion, underplating and arc volcanism along the margin of Costa Rica: Constraints from Ba, Zn, Ni, and ¹⁰Be concentrations, *EOS Trans. AGU* 78: 673.
- Weyl, R. 1980. *Geology of Central America*. Gebruder Borntraeger, Berlin, 371p.
- Woodhead, JD, Eggins, SM, Johnson, RW, 1998. Magma genesis in New Britain island arc; further insights into the melting and mass transfer processes *Journal of Petrology* 39: 1641-1668.

MICHIGAN STATE UNIVERSITY LIBRARIES



3 1293 02736 6974